

Structured Storage Policies for Energy Distribution Networks

Arnab Bhattacharya¹ Jeffrey P. Kharoufeh² Bo Zeng³

Department of Industrial Engineering

University of Pittsburgh

1025 Benedum Hall

3700 O'Hara Street

Pittsburgh, PA 15261 USA

Accepted Version

February 7, 2018

To appear in *IIEE Transactions*

Abstract

We consider the problem of dynamically controlling a 2-bus energy distribution network with energy storage capabilities. An operator seeks to dynamically adjust the amount of energy to charge to, or discharge from, energy storage devices in response to randomly-evolving demand, renewable supply and prices. The objective is to minimize the expected total discounted costs incurred within the network over a finite planning horizon. We formulate a Markov decision process (MDP) model that prescribes the optimal amount of energy to charge or discharge and transmit between the two buses during each stage of the planning horizon. Established are the multimodularity of the value function, and the monotonicity of the optimal policy, in the energy storage levels. We also show that the optimal operational cost is convex and monotone in the storage capacities. Furthermore, we establish bounds on the optimal cost by analyzing comparable single-storage systems with pooled and decentralized storage configurations, respectively. These results extend to more general multi-bus network topologies. Numerical examples illustrate the main results and highlight the significance of interacting demand-side entities.

Keywords: Energy storage; network; Markov decision processes.

¹Ph: 412-626-1799; Email: cfcarnabiitkgp@gmail.com

²Corresponding author. Ph: 412-624-9832; Email: jkharouf@pitt.edu

³Ph: 412-624-5045; Email: bzeng@pitt.edu

1 Introduction

Despite energy efficiency improvements and targeted efforts to reduce residential energy consumption, the U.S. Energy Information Administration (EIA) predicts a 24% increase in U.S. residential electricity demand by the year 2040, while electricity prices are expected to rise by over 13% over the same period [1]. If realized, these increases will impose enormous pressure on the electric power grid to produce reliable and sustainable energy. The integration of renewable energy sources, such as wind and solar power, into the main grid will likely play a prominent role in meeting the escalating demand for electricity. Indeed, the EIA forecasts that renewable sources will account for roughly 57% of the increase in power generation between 2010 and 2030, and that renewable energy will comprise no less than 15% of the overall generation portfolio by 2030 [15].

One way to increase the penetration of renewable sources is to integrate small-scale, distributed generation (DG) sources, such as solar panels or wind turbines, in close proximity to local consumer demand [29, 48]. In addition to satisfying local demand, DG sources also provide ancillary services, such as reactive capacity and spinning reserves, to the main grid. However, the intermittent and variable nature of DG sources may significantly affect the availability of energy within a distribution network, as DG sources have limited generating capacities in the range of 1-1000 kilowatts (kW) and are highly susceptible to power reliability issues. Moreover, a high penetration of DG sources increases the risk of short-circuit faults and voltage fluctuations in distribution networks [13], which can severely impact the quality of energy supplied to local consumers. Presumably, these complications can be overcome by deploying small-scale, distributed energy storage (DES) systems, such as batteries and flywheels, with storage capacities in the range 5-100 kilowatt-hours (kW-h). Energy storage can be used to decouple the times of energy consumption and generation, thereby enabling network operators to improve energy generation and scheduling decisions in distribution networks. With the advent of bidirectional communication technologies, operators can exploit arbitrage opportunities in electricity markets by storing energy in low-price periods for use in peak-price periods – often referred to as *time-shifting of energy* [24, 35, 46, 48, 51, 55]. Finally, DES systems help curtail the dependence on polluting ancillary sources (e.g., diesel fuel generators) [17, 25] and promote sustainable and clean energy usage in distribution networks.

In this paper, we examine optimal energy storage management strategies in power networks with access to local renewable DG sources, as well as finite-capacity DES devices. The network operator’s objective is to minimize the expected total discounted costs incurred over a finite planning horizon by making a sequence of operational decisions. Specifically, for each stage of the planning horizon, the operator must decide (i) the amount of energy to charge to, or discharge from, the energy storage devices; and (ii) the amount of energy to transmit between the load buses. These decisions are complicated by uncertainty in local demand, the supply of renewable energy and the real-time price of electricity. Furthermore, the operator must balance supply and demand, while considering storage inefficiencies and line losses. To address the operator’s problem, we devise a finite-horizon, discounted Markov decision process (MDP) model and analyze its key attributes.

Energy storage, as a means by which to integrate renewable sources into the power grid, has

spawned significant interest in the energy systems modeling literature. The storage problem bears some resemblance to classical inventory and asset management problems (cf. [16, 59]), except that the operator is faced with multiple sources of uncertainty, storage and line inefficiencies, as well as network energy balance constraints. Most of the relevant work in this area focuses on devising an optimal storage policy for a single consumer (or supplier) with access to renewable energy and finite-capacity storage. A linear programming approach was employed to solve the consumer’s storage problem under deterministic price, demand and renewable supply levels in [2, 23]. Bar-Noy et al. [6, 7] developed efficient online algorithms to reduce a consumer’s peak demand costs by optimally procuring and storing energy when demand is uncertain. More recently, MDP models have been used extensively to analyze the single consumer problem under exogenous uncertainty. Using an infinite-horizon MDP model, Van de Ven et al. [50] proved the existence of an optimal dual-threshold storage policy for a consumer with uncertain demands, subject to deterministic time-of-use electricity prices. Harsha and Dahleh [20] derived a similar dual-threshold optimal storage policy for a finite-horizon problem under uncertain prices, demand and renewable supply. Furthermore, they analytically characterize a consumer’s optimal storage capacity for the case when prices are fixed. Similar single-storage MDP models have been employed for a supplier’s storage management problem, which involves optimizing the bidding strategies of renewable suppliers that participate in day-ahead or real-time energy markets to maximize profits by deploying energy storage (cf. [10, 12, 18, 26, 27, 28, 34, 42, 56]). However, single-storage models do not account for network constraints and interactions between different network entities with storage, rendering them unrealistic for our setting. Alternatively, stochastic programming (SP) models have been devised to solve network storage problems with continuous actions and high-dimensional state spaces. Some representative examples of such models include [9, 18, 30, 36, 53]. Although SP models allow for the incorporation of network constraints, the number of possible scenarios in such models can be prohibitively large. Additionally, solutions to SP models can be difficult to interpret, as they provide little insight into the structure of the optimal policy.

The model we present here is distinguished from existing single-storage models in that it considers the perspective of multiple demand-side entities, each with energy storage capabilities, in a distribution network. Specifically, we first examine a 2-bus network model in which decisions are made under randomly-evolving demand, renewable supply and real-time electricity prices. This model captures the salient features of distributed energy storage operations by considering the impact of renewable generation, storage inefficiencies, supply-demand imbalances, distribution energy losses, and constrained power-line capacities on the optimal storage decisions. We focus first on the 2-bus system in light of the fact that network reduction methods can be used to analyze more complicated multi-bus networks as equivalent 2-bus networks for power system planning and operational problems [38, 41, 52]. A unique feature of our model is the fact that the buses can transmit energy to one another – a feature that is shown to significantly impact the optimal decisions and operational costs. Our main results can be summarized as follows. First, we establish the monotonicity and convexity of our MDP model’s value function in the storage levels for each fixed exogenous state. Next, we prove that the value function is multimodular in the storage levels,

the optimal policy is monotone and the optimal storage decisions in each stage exhibit bounded sensitivities. We also establish bounds that compare the cost of the 2-bus network to those of two comparable systems with pooled and decentralized storage configurations, respectively, and the main results are extended to more general multi-bus network topologies. To illustrate the structural properties, we present numerical examples that use real renewable generation and pricing data obtained from open sources. These examples help quantify the benefits of using the network model in lieu of simpler, single-storage models that fail to account for interactions between demand-side entities in a distribution network.

The remainder of the paper is organized as follows. The next section describes the 2-bus distribution network and introduces notation and nomenclature of the mathematical model. In Section 3, we present the main results, which include structural properties of the value function, optimal policy and the optimal operational cost. Section 4 provides numerical examples that illustrate the main structural results and highlight the importance of interactions between network entities. Finally, in Section 5, we provide a few concluding remarks and directions for future work.

2 Model Description

Consider a 2-bus network connected to the main grid through a reference bus (or *feeder*) as depicted in Figure 1. The feeder is not connected to any distributed energy storage system or renewable energy sources; however, the other two buses (the *load buses*) are connected to finite-capacity storage systems and renewable generators that satisfy the demand realized at these buses. Any unmet demand can be satisfied by procuring energy from the grid and/or by receiving energy transmitted from the other bus. Similarly, any surplus energy generated at a load bus can be sold to the main grid and/or transmitted to the other load bus. However, energy flow between the buses is constrained by the capacity of the power line (hereafter the *line*) connecting them, as well as supply-demand balance constraints at each bus. Additionally, storage capacity limitations restrict the amount of energy that can be charged to, or discharged from, the storage devices. We assume that a central network operator (or controller) is responsible for all energy flow and storage decisions within the distribution network.

The distribution network incurs three types of costs: *(i)* the explicit cost of procuring energy from, or selling energy to, the grid at real-time prices; *(ii)* the implicit cost of lost energy due to line losses stemming from resistive overheating [4]; and *(iii)* costs associated with storage inefficiencies. While transmitting energy between the load buses helps to offset the cost of procuring energy from the grid, only a limited amount of energy can be transmitted due to a line capacity constraint between the buses. Moreover, transmitting stored energy to another bus is a lost opportunity to procure and store surplus energy from the grid for future use when prices are high. Therefore, an obvious tradeoff exists between the amount of energy to buy or sell, and the amount that is transmitted between the load buses. The operator’s objective is to minimize the expected total discounted costs incurred over a finite planning horizon by making a sequence of operational decisions. For each stage of the planning horizon, the operator must decide the amount of energy to:

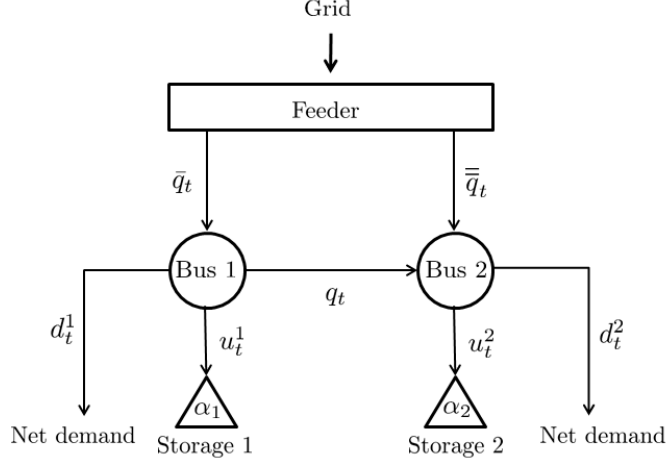


Figure 1: Graphical depiction of a 2-bus distribution network.

(i) buy from, or sell to, the main grid; (ii) charge to, or discharge from, the energy storage devices; and (iii) transmit between the two load buses. These decisions are made under randomly-varying demand, renewable generation and real-time prices.

We formulate the operator's sequential decision problem using a finite-horizon Markov decision process (MDP) model. Specifically, consider a planning horizon of length Υ and partition the time interval $[0, \Upsilon)$ so that

$$[0, \Upsilon) = \bigcup_{t=1}^N [\varepsilon_{t-1}, \varepsilon_t),$$

where N is the number of time intervals (or stages) and ε_t is the t th decision epoch with $\varepsilon_0 \equiv 0$ and $\varepsilon_N \equiv \Upsilon$. The discrete time horizon is denoted by $T = \{1, 2, \dots, N\}$, where $t \in T$ is the index of the t th stage, namely the interval $[\varepsilon_{t-1}, \varepsilon_t)$. It is assumed that no decisions are made at stage N . For future use, let $T' \equiv T \setminus \{N\}$. Let $C = \{0, 1, 2\}$ be the set of buses in the network, where bus 0 is the feeder, and bus $i \in C' \equiv \{1, 2\}$ denotes the i th load bus. The set of all lines in the network is denoted by $A = \{(i, j) : i, j \in C\}$, where (i, j) is the line connecting bus i to bus j .

The physical parameters of the network are described as follows. Let α_i ($\alpha_i < \infty$) denote the capacity of the storage device located at bus $i \in C'$. The parameters ρ_c^i and ρ_d^i denote the charging and discharging efficiencies of the storage device at bus i , where $\rho_c^i, \rho_d^i \in (0, 1]$. The round-trip efficiency of the storage device at bus i is defined as $\rho_i \equiv \rho_c^i \rho_d^i$. The quantities τ_c^i and τ_d^i denote the maximum charging and discharging rates of the storage device at bus i , respectively. Gather the parameters α_i , τ_c^i and τ_d^i in the vectors $\boldsymbol{\alpha}$, $\boldsymbol{\tau}_c$ and $\boldsymbol{\tau}_d$, respectively. Let β be the capacity of the line connecting the load buses. Finally, let ν denote the per-unit cost of line losses, while φ is the per-unit cost of charging energy to, or discharging energy from, the storage devices.

The model contains several sources of uncertainty that we now describe in detail. All random variables are defined on a common, complete and filtered probability space $(\Omega, \mathcal{A}, \{\mathcal{A}_t\}_{t \in \mathcal{T}}, \mathbb{P})$ with natural filtration $\{\mathcal{A}_t : t \in \mathcal{T}\}$, i.e., \mathcal{A}_t contains the information available up to stage t . Any random quantity with subscript t is assumed to be \mathcal{A}_t -measurable. Let D_t^i denote the random

net demand (demand minus renewable supply) at bus $i \in C'$ with countable support $\mathcal{D}_t^i \subset \mathbb{R}$, and let P_t be the random real-time price at the start of stage t with countable support $\mathcal{P}_t \subset \mathbb{R}_+$. Let $\mathbf{W}_t = (P_t, D_t^1, D_t^2)$ denote the *exogenous* information available at the start of stage t , and let $\mathcal{W}_t \equiv \mathcal{P}_t \times \mathcal{D}_t^1 \times \mathcal{D}_t^2$ be the support of \mathbf{W}_t . A realization of \mathbf{W}_t is denoted by $\mathbf{w}_t \equiv (p_t, d_t^1, d_t^2)$, where p_t, d_t^1 and d_t^2 are realizations of P_t, D_t^1 and D_t^2 , respectively. This information is exogenous in the sense that the evolution of \mathbf{W}_t is independent of the operator's decisions over the planning horizon. The set of all sample paths of $\mathbf{W} = \{\mathbf{W}_t : t \in T\}$ is denoted by $\mathcal{W} \equiv \mathcal{W}_1 \times \cdots \times \mathcal{W}_N$, and it is assumed that \mathbf{W} possesses the Markov property, i.e., for any $t \in T$,

$$\mathbb{P}(\mathbf{W}_t = \mathbf{w}_t | \mathbf{W}_{t-1}, \dots, \mathbf{W}_1; \mathcal{A}_{t-1}) = \mathbb{P}(\mathbf{W}_t = \mathbf{w}_t | \mathbf{W}_{t-1}; \mathcal{A}_{t-1}), \quad \mathbf{w}_t \in \mathcal{W}_t.$$

At the start of stage t , let the (random) storage level at bus i be denoted by Y_t^i , define $\mathbf{Y}_t = (Y_t^1, Y_t^2)$ and let $\mathcal{Y} \equiv [0, \alpha_1] \times [0, \alpha_2]$ be the set of all possible storage levels. Note that \mathcal{Y} is time-invariant, as the storage capacities α_1 and α_2 are fixed *a priori*. In contrast to the exogenous variables, the endogenous component \mathbf{Y}_t is influenced by the operator's actions up to stage $t - 1$. The random state of the process at the start of stage t is a vector $\mathbf{S}_t = (\mathbf{W}_t, \mathbf{Y}_t)$ whose state space is $\mathcal{S}_t \equiv \mathcal{W}_t \times \mathcal{Y}$. A realization of \mathbf{S}_t is denoted by $\mathbf{s}_t = (\mathbf{w}_t, \mathbf{y}_t)$ for $\mathbf{w}_t \in \mathcal{W}_t$ and $\mathbf{y}_t \in \mathcal{Y}$, and we assume that the initial state, \mathbf{S}_1 , is known with certainty.

The decision process evolves as follows. At the start of each stage, the operator observes the exogenous state and the current storage levels at the load buses. Then, the operator makes the operational decisions to procure or sell, to charge or discharge, and whether to transmit energy between the load buses. The operator makes no decisions in the final stage and incurs a terminal cost. It is noted that all of the decisions are made simultaneously because, unlike other commodities, energy cannot be backlogged and needs to be consumed immediately. Let $\mathbf{x}_t(\mathbf{s}_t)$ be the decision vector at the start of stage t when state \mathbf{s}_t is realized; henceforth, the dependence of \mathbf{x}_t on \mathbf{s}_t is suppressed for notational brevity. The decision vector \mathbf{x}_t assumes the form $\mathbf{x}_t = (\mathbf{u}_t, q_t)$, where the vector \mathbf{u}_t contains the charge/discharge decisions at each bus, and q_t is the amount of energy to transmit between the buses. Note that the buy/sell decisions are not explicitly included in the decision vector, as these decisions are auxiliary to the charge/discharge decisions. These quantities are further elucidated in what follows, along with the feasibility set of \mathbf{x}_t .

Let $\mathbf{u}_t = (u_t^i : i \in C')$ be the vector of charging/discharging decisions at stage t described as follows. For each stage t : (i) if $u_t^i > 0$, then u_t^i units of energy are charged to the storage device at bus i ; (ii) if $u_t^i < 0$, then $-u_t^i$ units of energy are discharged from the storage device at bus i ; and (iii) if $u_t^i = 0$, then energy is neither charged to, nor discharged from, the storage device at bus i . The charging/discharging decisions are constrained by the storage capacities and the charging/discharging rates of the storage devices. That is,

$$-\min\{\mathbf{y}_t, \boldsymbol{\tau}_d\} \leq \mathbf{u}_t \leq \min\{\boldsymbol{\alpha} - \mathbf{y}_t, \boldsymbol{\tau}_c\}, \quad t \in T', \quad (1)$$

where all inequalities involving vectors are understood to hold component-wise.

The energy flow between the buses at stage t , namely q_t , is described as follows: if $q_t > 0$, then q_t units of energy flow from bus 1 to bus 2; if $q_t < 0$, then $-q_t$ units of energy flow from bus 2 to

bus 1; and if $q_t = 0$, then no energy flows between the two buses. These variables are constrained by the line capacity via

$$-\beta \leq q_t \leq \beta, \quad t \in T'. \quad (2)$$

Similarly, let g_t^1 and g_t^2 be the energy flow in the lines connecting the feeder to buses 1 and 2 (the *feeder lines*), respectively. Here, if $g_t^1, g_t^2 > 0$, then energy flows from the feeder to the load buses, and if $g_t^1, g_t^2 < 0$, energy flows from the buses to the feeder. If these quantities are zero, then no energy is bought from, or sold to, the grid. For each $t \in T'$ and $i \in C'$, define the variables θ_t^i as follows:

$$\theta_t^i = \begin{cases} 1/\rho_c^i, & u_t^i \geq 0, \\ \rho_d^i, & u_t^i < 0. \end{cases}$$

Then the supply-demand balance equations at the load buses are

$$g_t^1 = d_t^1 + \theta_t^1 u_t^1 + q_t, \quad t \in T', \quad (3)$$

$$g_t^2 = d_t^2 + \theta_t^2 u_t^2 - q_t, \quad t \in T'. \quad (4)$$

As noted earlier, g_t^1 and g_t^2 are auxiliary variables that depend on (\mathbf{u}_t, q_t) and represent the buying/selling decisions. Because the feeder lines serve as the main connection between the distribution system and the main grid, they typically possess sufficient, reliable capacity and incur only minor line losses. Therefore, we assume that energy flows in the feeder lines are not restricted by line capacities and do not incur line losses. Next, define the stage t feasibility set (or action space) by $\mathcal{X}_t(\mathbf{y}_t)$, which is characterized by the linear constraints (1) and (2); note that $\mathcal{X}_t(\mathbf{y}_t)$ is a bounded polyhedron. A feasible policy is a vector $\boldsymbol{\pi} = (\mathbf{x}_t : t \in T') \in \Pi$, where Π denotes the set of all feasible Markov deterministic (MD) policies.

Following the actions taken by the operator in the current stage, the process next transitions randomly to another state in the next stage. The endogenous storage levels evolve as a deterministic function of the current storage levels and the charge/discharge decisions via

$$\mathbf{y}_{t+1} = \mathbf{y}_t + \mathbf{u}_t, \quad t \in T', \quad (5)$$

while the exogenous variables evolve according to the non-stationary, conditional probability distribution $\mathbb{P}_t(\mathbf{w}_{t+1}|\mathbf{w}_t)$. The transition probabilities of the Markov chain induced by $\boldsymbol{\pi}$ are

$$\mathbb{P}_t^\pi(\mathbf{s}_{t+1}|\mathbf{s}_t) = \psi(\mathbf{y}_{t+1} - \mathbf{y}_t - \mathbf{u}_t) \mathbb{P}_t(\mathbf{w}_{t+1}|\mathbf{w}_t), \quad t \in T', (\mathbf{s}_t, \mathbf{s}_{t+1}) \in \mathcal{S}_t \times \mathcal{S}_{t+1}, \quad (6)$$

where $\psi(\mathbf{a})$ is the Kronecker-delta function, i.e., for $\mathbf{a} \in \mathbb{R}^n$, $\psi(\mathbf{a}) = 1$ when $\mathbf{a} = \mathbf{0}$, and $\psi(\mathbf{a}) = 0$ otherwise.

Next, we describe the objective function which is the cost to be minimized. The one-step cost incurred in stage t is

$$c_t(\mathbf{s}_t, \mathbf{x}_t) = p_t(g_t^1 + g_t^2) + \varphi(|u_t^1| + |u_t^2|) + \nu\xi(\mathbf{u}_t, q_t), \quad t \in T', \quad (7)$$

and $c_N(\mathbf{s}_N) = 0$ without loss of generality. The first term on the right-hand side (r.h.s.) of (7) is the total cost of procuring or selling energy, the second term is the total cost of charging or

discharging energy, and the third term is the cost of resistive line losses, where ξ , the resistive line-loss function, is nonnegative, separable and convex in (\mathbf{u}_t, q_t) (see [9, 47]). It is assumed that $|c_t(\mathbf{s}_t, \mathbf{x}_t)| < \infty$. For an *a priori* storage configuration $\boldsymbol{\alpha}$, the operator seeks an optimal policy $\boldsymbol{\pi}^* \in \Pi$ that minimizes the expected total discounted costs over the planning horizon as follows:

$$z_{\boldsymbol{\alpha}} = \min_{\boldsymbol{\pi} \in \Pi} \mathbb{E}_{\mathbf{s}}^{\boldsymbol{\pi}} \left(\sum_{t \in T'} \delta^{t-1} c_t(\mathbf{s}_t, \mathbf{x}_t) \middle| \mathbf{S}_1 = \mathbf{s}; \boldsymbol{\alpha} \right), \quad (8)$$

where $\delta \in (0, 1]$ is a discount factor. Henceforth, we call $z_{\boldsymbol{\alpha}}$ the optimal operational cost. Bellman's optimality equations are then

$$V_t(\mathbf{s}_t) = \min_{\mathbf{x}_t \in \mathcal{X}_t(\mathbf{y}_t)} c_t(\mathbf{s}_t, \mathbf{x}_t) + \delta \mathbb{E}(V_{t+1}(\mathbf{s}_{t+1}) | \mathbf{s}_t, \mathbf{x}_t), \quad t \in T', \quad (9)$$

with $V_N(\mathbf{s}_N) = 0$.

3 Structural Results

In this section, we present important structural properties of the value function, V_t , the optimal policy $\boldsymbol{\pi}^*$ and the optimal cost $z_{\boldsymbol{\alpha}}$. First, we examine properties of V_t that depend on the exogenous component \mathbf{w}_t and the endogenous storage levels \mathbf{y}_t . Subsequently, we examine the behavior of the optimal policy. In what follows, a fixed exogenous state is denoted by $\bar{\mathbf{w}}_t$.

3.1 Structural Properties of the Value Function

In this subsection, we examine important properties of the value function V_t . First note that, for a fixed exogenous state $\bar{\mathbf{w}}_t$, the function $c_t(\bar{\mathbf{w}}_t, \mathbf{y}_t, \mathbf{x}_t)$ is convex in $(\mathbf{y}_t, \mathbf{x}_t)$. Proposition 1 asserts that the expected future cost at each stage is jointly convex in the storage levels. Stated more clearly, the marginal cost of using storage increases with increasing storage levels.

Proposition 1 *For each $t \in T$, $V_t(\bar{\mathbf{w}}_t, \mathbf{y}_t)$ is convex in $\mathbf{y}_t \in \mathcal{Y}$.*

Proof. The result is proved using backward induction on $V_t(\mathbf{w}_t, \mathbf{y}_t)$ for a fixed \mathbf{w}_t . By assumption, $V_N(\mathbf{s}_N) = 0$ for all $\mathbf{s}_N \in \mathcal{S}_N$, so the result clearly holds at stage N . For the induction hypothesis, suppose $V_{t+1}(\mathbf{w}_{t+1}, \mathbf{y}_{t+1})$ is convex in \mathbf{y}_{t+1} , given a fixed \mathbf{w}_{t+1} , for $t + 1 < N$. Note that the expectation in (9) is taken with respect to (w.r.t.) the conditional probability distribution $\mathbb{P}_t(\mathbf{w}_{t+1} | \bar{\mathbf{w}}_t)$. Moreover, \mathbf{y}_{t+1} is a linear, deterministic function of \mathbf{y}_t and \mathbf{u}_t by (5). Therefore, the expectation in (9) can be expressed around the post-decision state $\mathbf{s}_t^x = (\bar{\mathbf{w}}_t, \mathbf{y}_t + \mathbf{u}_t)$ (see [39] for additional details), so that

$$V_t(\bar{\mathbf{w}}_t, \mathbf{y}_t) = \min_{\mathbf{x}_t \in \mathcal{X}_t(\mathbf{y}_t)} c_t(\bar{\mathbf{w}}_t, \mathbf{x}_t) + V_t^x(\bar{\mathbf{w}}_t, \mathbf{y}_t + \mathbf{u}_t), \quad (10)$$

where $V_t^x(\bar{\mathbf{w}}_t, \mathbf{y}_t + \mathbf{u}_t) \equiv \delta \mathbb{E}(V_{t+1}(\mathbf{s}_{t+1} | \mathbf{s}_t^x))$ is the post-decision value function. As the expectation operator preserves convexity, and compositions of convex and affine functions are also convex (see

Proposition 2.1.3 (b) of [45]), $V_t^x(\bar{\mathbf{w}}_t, \mathbf{y}_t + \mathbf{u}_t)$ is convex in $(\mathbf{y}_t, \mathbf{u}_t)$. Note that an optimal solution to (10) exists because $\mathcal{X}_t(\mathbf{y}_t)$ is a bounded polyhedron. Moreover, $c_t(\bar{\mathbf{w}}_t, \mathbf{x}_t)$ is piecewise-convex in \mathbf{x}_t . As the sum of two convex functions is convex, the objective function of (10) is jointly convex in $(\mathbf{y}_t, \mathbf{x}_t)$. As convexity is preserved under partial minimization (see Section 3.2.5 in [11]), we conclude that $V_t(\bar{\mathbf{w}}_t, \mathbf{y}_t)$ is convex in \mathbf{y}_t . ■

Intuitively, Proposition 1 implies that the flexibility to store surplus generation decreases with an increase in the current storage level. Consequently, the operator must either sell the excess energy, possibly at a lower price, or transmit a portion of it to the other bus, possibly incurring line-loss costs. Note that, if the functional form of V_t is known for a fixed $\bar{\mathbf{w}}_t$, the optimality equations (9) can be solved efficiently using convex optimization algorithms. Unfortunately, characterizing the expectation in (9) is nontrivial due to the multidimensional nature of \mathcal{S}_t and $\mathcal{X}_t(\mathbf{y}_t)$.

The next result, Proposition 2, asserts that the expected future cost at each stage is monotone decreasing in the storage levels.

Proposition 2 *For each $t \in T$, $V_t(\bar{\mathbf{w}}_t, \mathbf{y}_t)$ is monotone decreasing in $\mathbf{y}_t \in \mathcal{Y}$.*

Proof. The proposition is proved via backward induction on $V_t(\mathbf{w}_t, \mathbf{y}_t)$ for a fixed \mathbf{w}_t . Clearly, the result holds at stage N . For the induction hypothesis, suppose $V_{t+1}(\mathbf{w}_{t+1}, \mathbf{y}_{t+1})$ is monotone decreasing in \mathbf{y}_{t+1} for $t+1 < N$ for a fixed \mathbf{w}_{t+1} . As the expectation operator preserves monotonicity, the function $V_t^x(\bar{\mathbf{w}}_t, \mathbf{y}_t + \mathbf{u}_t)$ in (10) is decreasing in \mathbf{y}_t and \mathbf{u}_t . Next, consider two states $\mathbf{s}_t^a = (\bar{\mathbf{w}}_t, \mathbf{y}_t^a)$ and $\mathbf{s}_t^b = (\bar{\mathbf{w}}_t, \mathbf{y}_t^b)$, such that $0 \leq \mathbf{y}_t^a < \mathbf{y}_t^b \leq \boldsymbol{\alpha}$. We seek to show that $V_t(\bar{\mathbf{w}}_t, \mathbf{y}_t^a) \geq V_t(\bar{\mathbf{w}}_t, \mathbf{y}_t^b)$. To this end, let $\mathbf{x}_t^a = (\mathbf{u}_t^a, q_t^a)$ and $\mathbf{x}_t^b = (\mathbf{u}_t^b, q_t^b)$ be the optimal solutions of (10) for states \mathbf{s}_t^a and \mathbf{s}_t^b , respectively. Then,

$$\begin{aligned} V_t(\bar{\mathbf{w}}_t, \mathbf{y}_t^a) &= c_t(\bar{\mathbf{w}}_t, \mathbf{u}_t^a, q_t^a) + V_t^x(\bar{\mathbf{w}}_t, \mathbf{y}_t^a + \mathbf{u}_t^a), \\ V_t(\bar{\mathbf{w}}_t, \mathbf{y}_t^b) &= c_t(\bar{\mathbf{w}}_t, \mathbf{u}_t^b, q_t^b) + V_t^x(\bar{\mathbf{w}}_t, \mathbf{y}_t^b + \mathbf{u}_t^b). \end{aligned}$$

Consider the following two cases:

Case 1: Suppose $\mathbf{x}_t^a \in \mathcal{X}_t(\mathbf{y}_t^b)$. As \mathbf{x}_t^a is feasible for problem (10) in state \mathbf{s}_t^b , the optimal value $V_t(\bar{\mathbf{w}}_t, \mathbf{y}_t^b)$ is at most equal to the objective value at \mathbf{x}_t^a , i.e.,

$$c_t(\bar{\mathbf{w}}_t, \mathbf{u}_t^a, q_t^a) + V_t^x(\bar{\mathbf{w}}_t, \mathbf{y}_t^b + \mathbf{u}_t^a) \geq V_t(\bar{\mathbf{w}}_t, \mathbf{y}_t^b). \quad (11)$$

As $\mathbf{y}_t^a < \mathbf{y}_t^b$, the following inequality holds by the induction hypothesis on V_t^x :

$$V_t^x(\bar{\mathbf{w}}_t, \mathbf{y}_t^a + \mathbf{u}_t^a) \geq V_t^x(\bar{\mathbf{w}}_t, \mathbf{y}_t^b + \mathbf{u}_t^a). \quad (12)$$

Adding $c_t(\bar{\mathbf{w}}_t, \mathbf{u}_t^a, q_t^a)$ to both sides of (12) and combining it with (11) yields

$$c_t(\bar{\mathbf{w}}_t, \mathbf{u}_t^a, q_t^a) + V_t^x(\bar{\mathbf{w}}_t, \mathbf{y}_t^a + \mathbf{u}_t^a) \geq c_t(\bar{\mathbf{w}}_t, \mathbf{u}_t^a, q_t^a) + V_t^x(\bar{\mathbf{w}}_t, \mathbf{y}_t^b + \mathbf{u}_t^a) \geq V_t(\bar{\mathbf{w}}_t, \mathbf{y}_t^b), \quad (13)$$

where the left-most expression in (13) equals $V_t(\bar{\mathbf{w}}_t, \mathbf{y}_t^a)$ by definition. Hence, $V_t(\bar{\mathbf{w}}_t, \mathbf{y}_t^a) \geq V_t(\bar{\mathbf{w}}_t, \mathbf{y}_t^b)$.

Case 2: Suppose $\mathbf{x}_t^a \notin \mathcal{X}_t(\mathbf{y}_t^b)$. A sufficient condition for $\mathbf{x}_t^a \notin \mathcal{X}_t(\mathbf{y}_t^b)$ is $\mathbf{u}_t^a \in (\boldsymbol{\alpha} - \mathbf{y}_t^b, \min\{\boldsymbol{\tau}_c, \boldsymbol{\alpha} - \mathbf{y}_t^a\}]$. Construct a feasible solution $\bar{\mathbf{x}}_t^b = (\bar{\mathbf{u}}_t^b, \bar{q}_t^b) \in \mathcal{X}_t(\mathbf{y}_t^b)$ such that $\bar{\mathbf{u}}_t^b = \boldsymbol{\alpha} - \mathbf{y}_t^b < \mathbf{u}_t^a$ and $\bar{q}_t^b = q_t^a$. For such a case,

$$\begin{aligned} V_t(\bar{\mathbf{w}}_t, \mathbf{y}_t^a) &= c_t(\bar{\mathbf{w}}_t, \mathbf{u}_t^a, q_t^a) + V_t^x(\bar{\mathbf{w}}_t, \mathbf{y}_t^a + \mathbf{u}_t^a) \geq c_t(\bar{\mathbf{w}}_t, \bar{\mathbf{u}}_t^b, \bar{q}_t^b) + V_t^x(\bar{\mathbf{w}}_t, \mathbf{y}_t^a + \mathbf{u}_t^a) \\ &\geq c_t(\bar{\mathbf{w}}_t, \bar{\mathbf{u}}_t^b, \bar{q}_t^b) + V_t^x(\bar{\mathbf{w}}_t, \boldsymbol{\alpha}) \\ &\geq c_t(\bar{\mathbf{w}}_t, \mathbf{u}_t^b, q_t^b) + V_t^x(\bar{\mathbf{w}}_t, \mathbf{y}_t^b + \mathbf{u}_t^b) \\ &= V_t(\bar{\mathbf{w}}_t, \mathbf{y}_t^b). \end{aligned}$$

The first inequality holds because $c_t(\bar{\mathbf{w}}_t, \mathbf{u}_t^a, q_t^a) \geq c_t(\bar{\mathbf{w}}_t, \bar{\mathbf{u}}_t^b, \bar{q}_t^b)$ for $\mathbf{u}_t^a > \bar{\mathbf{u}}_t^b$ and $q_t^a = \bar{q}_t^b$. The second inequality holds by the induction hypothesis on V_t^x . The third inequality holds because $(\bar{\mathbf{u}}_t^b, \bar{q}_t^b)$ is a feasible, but not necessarily optimal, solution to problem (10) for state \mathbf{s}_t^b . Hence, we conclude that $V_t(\bar{\mathbf{w}}_t, \mathbf{y}_t^a) \geq V_t(\bar{\mathbf{w}}_t, \mathbf{y}_t^b)$, and the proof is complete. \blacksquare

Proposition 2 suggests that stored energy tends to reduce the expected operational costs. When the storage levels are high, a larger fraction of the demand is satisfied by using stored energy, thereby reducing the overall operational cost. Moreover, higher storage levels allow the operator to satisfy demand and sell any excess energy back to the grid. This is especially useful during the peak-price, peak-demand periods.

Next, we present a result for the special case in which the load buses have similar operational characteristics. The load buses are called homogenous if: (i) $\alpha_1 = \alpha_2$, and (ii) the (conditional) joint cumulative distribution function (c.d.f.) of the net demands at each stage is *symmetric*, i.e., for $t \in T$, $k \in \{t, \dots, N\}$ and any $a_1, a_2 \in \mathbb{R}$,

$$\mathbb{P}_k(D_{k+1}^1 \leq a_1, D_{k+1}^2 \leq a_2 | \mathbf{D}_k; \mathcal{A}_k) = \mathbb{P}_k(D_{k+1}^1 \leq a_2, D_{k+1}^2 \leq a_1 | \mathbf{D}_k; \mathcal{A}_k). \quad (14)$$

Condition (14) is indicative of a joint distribution function in \mathbb{R}^2 that is symmetric along the line $a_1 = a_2$. Proposition 3 asserts that, for a pair of homogenous buses, allocating the total stored energy equally between the two buses minimizes the expected future cost at each stage. For ease of exposition, let $\mathcal{Y}_t^\Theta \equiv \{\mathbf{y}_t \in \mathcal{Y} : y_t^1 + y_t^2 = \Theta\}$ denote the set of feasible storage-level allocations at stage t when the total stored energy in the network is $\Theta \in [0, \alpha_1 + \alpha_2]$.

Proposition 3 For each $t \in T$ and a fixed Θ ,

$$V_t(\bar{\mathbf{w}}_t, \mathbf{y}_t) \geq V_t(\bar{\mathbf{w}}_t, \Theta/2), \quad \forall \mathbf{y}_t \in \mathcal{Y}_t^\Theta.$$

Proof. The result obviously holds at stage N . For $t \in T'$, consider two feasible storage-level vectors \mathbf{y}_t^a and \mathbf{y}_t^b , such that $\mathbf{y}_t^a, \mathbf{y}_t^b \in \mathcal{Y}_t^\Theta$. By definition, $(\mathbf{y}_t^a + \mathbf{y}_t^b)/2 = (\Theta/2, \Theta/2) \equiv \Theta/2$. For a pair of homogenous buses that satisfy the conditions $\alpha_1 = \alpha_2$ and (14), it follows directly that V_t is symmetric w.r.t. \mathbf{y}_t for a fixed $\bar{\mathbf{w}}_t$, i.e., $V_t(\bar{\mathbf{w}}_t, \mathbf{y}_t^a) = V_t(\bar{\mathbf{w}}_t, \mathbf{y}_t^b)$. Using Jensen's inequality for the convex function V_t at the points $\mathbf{y}_t = \mathbf{y}_t^a$ and $\mathbf{y}_t = \mathbf{y}_t^b$, we obtain

$$V_t(\bar{\mathbf{w}}_t, \mathbf{y}_t^a) = \frac{1}{2} \left(V_t(\bar{\mathbf{w}}_t, \mathbf{y}_t^a) + V_t(\bar{\mathbf{w}}_t, \mathbf{y}_t^b) \right) \geq V_t(\bar{\mathbf{w}}_t, (\mathbf{y}_t^a + \mathbf{y}_t^b)/2) = V_t(\bar{\mathbf{w}}_t, \Theta/2, \Theta/2).$$

As \mathbf{y}_t^a (or \mathbf{y}_t^b) is any feasible element in \mathcal{Y}_t^Θ , we conclude that $V_t(\bar{\mathbf{w}}_t, \mathbf{y}_t) \geq V_t(\bar{\mathbf{w}}_t, \Theta/2, \Theta/2)$ for all $\mathbf{y}_t \in \mathcal{Y}_t^\Theta$. \blacksquare

3.2 Behavior of the Optimal Policy

Here we examine structural properties of the optimal policy π^* . For a fixed $\bar{\mathbf{w}}_t$, the optimality equations (9) are a collection of parameterized optimization problems in which the objective function and the constraints depend on the storage levels \mathbf{y}_t . For such a class of problems, *monotone comparative statics* [49] can be used to characterize the monotone behavior of optimal decisions with respect to the state variables. Moreover, monotone comparative statics are useful for problems in which the value function is non-differentiable [33] and are closely linked to the concept of *substitutability*. Two variables are called economic substitutes if an increase in one variable increases the marginal cost of the other variable [45]. The property of multimodularity [3, 19, 37] is known to imply substitutability, and is inherently related to the concepts of supermodularity and increasing differences that arise frequently in lattice theory [49]. In what follows, we show that, for a fixed $\bar{\mathbf{w}}_t$, V_t is multimodular in \mathbf{y}_t , and the optimal decisions \mathbf{x}_t^* are not only monotone, but also economic substitutes of \mathbf{y}_t . We first review some needed elements of lattice theory.

Consider $A \subset \mathbb{R}^n$ with the standard component-wise order \leq ; that is, for any $\mathbf{a}, \mathbf{a}' \in A$, $\mathbf{a} \leq \mathbf{a}'$ if and only if $a_i \leq a'_i$ for each $i = 1, \dots, n$. Any subset of \mathbb{R}^n is a partially-ordered set (or poset) by definition (see Section 2.2 of [49]). A special poset, namely a lattice, is a group-algebraic structure as next defined.

Definition 1 *A poset (A, \leq) is called a lattice if and only if for any $\mathbf{a}, \mathbf{a}' \in A$,*

$$\begin{aligned}\mathbf{a} \vee \mathbf{a}' &\equiv (\sup\{a_1, a'_1\}, \dots, \sup\{a_n, a'_n\}) \in A, \\ \mathbf{a} \wedge \mathbf{a}' &\equiv (\inf\{a_1, a'_1\}, \dots, \inf\{a_n, a'_n\}) \in A.\end{aligned}$$

In words, a lattice is a poset whose nonempty, finite subsets possess a supremum and an infimum. Given a lattice (A, \leq) , any $S \subseteq A$ is called a sublattice of A if S is itself a lattice. Note that \mathbb{R}^n is a lattice by definition. Next, we review important properties of functions defined on lattices.

Definition 2 *Let (A, \leq) be a lattice. A mapping $f : A \rightarrow \mathbb{R}$ is supermodular on A if for any $\mathbf{a}, \mathbf{a}' \in A$,*

$$f(\mathbf{a}) + f(\mathbf{a}') \leq f(\mathbf{a} \vee \mathbf{a}') + f(\mathbf{a} \wedge \mathbf{a}').$$

The function f is said to be submodular on A if $-f$ is supermodular on A .

Supermodular functions exhibit the more intuitive increasing differences property (see Theorem 2.2.2 in [45]). Given two posets (M, \leq) and (N, \leq) , a mapping $f : M \times N \rightarrow \mathbb{R}$ has increasing differences if for any $n, n' \in N$ with $n \leq n'$, $f(m, n') - f(m, n)$ is increasing in $m \in M$. Clearly, increasing differences, and therefore supermodularity, imply substitutability. However, supermodularity is not preserved under minimization [31, 45]. By contrast, multimodularity, which is next defined, is preserved under minimization [31, 58].

Definition 3 *Let $A = \{(\mathbf{v}, b) \in \mathbb{R}^{n+1} : (v_1 - b, v_2 - v_1, \dots, v_n - v_{n-1}) \in U \subseteq \mathbb{R}^n, b \in \mathbb{R}\}$ be a lattice characterized by the posets (U, \leq) and (\mathbb{R}, \leq) . A mapping $f : U \rightarrow \mathbb{R}$ is said to be multimodular on U if $\Psi(\mathbf{v}, b) \equiv f(v_1 - b, v_2 - v_1, \dots, v_n - v_{n-1})$ is submodular on A .*

Now, to establish the multimodularity of V_t , we first recast the sets \mathcal{Y} , $\mathcal{X}_t(\mathbf{y}_t)$ and $\mathcal{U} \equiv \mathcal{Y} \times \cup_{\mathbf{y}_t \in \mathcal{Y}} \mathcal{X}_t(\mathbf{y}_t)$ as lattices by employing the following change of variables: $y_t^1 = v_1 - b$, $y_t^2 = v_2 - v_1$, $u_t^1 = r_1 - v_1$, $u_t^2 = r_2 - v_2$, and $q_t = r_3 - r_2$, where $(\mathbf{v}, b) \equiv (v_1, v_2, b)$ and $\mathbf{r} \equiv (r_1, r_2, r_3)$ are vectors of new variables. Redefining the sets \mathcal{Y} , \mathcal{U} and $\mathcal{X}_t(\mathbf{y}_t)$, respectively, we obtain

$$\mathcal{V} \equiv \{(\mathbf{v}, b) \in \mathbb{R}^3 : v_1 - b \in [0, \alpha_1], v_2 - v_1 \in [0, \alpha_2]\}, \quad (15)$$

$$\mathcal{L} \equiv \{(\mathbf{v}, b, \mathbf{r}) \in \mathbb{R}^6 : (\mathbf{v}, b) \in \mathcal{V}, (r_1 - v_1, r_2 - v_2, r_3 - r_2) \in \mathcal{X}_t(v_1 - b, v_2 - v_1)\}, \quad (16)$$

$$\mathcal{L}(\mathbf{v}, b) \equiv \{\mathbf{r} \in \mathbb{R}^3 : (r_1 - v_1, r_2 - v_2, r_3 - r_2) \in \mathcal{X}_t(v_1 - b, v_2 - v_1)\}. \quad (17)$$

The set \mathcal{U} is the set of all feasible state-action pairs in stage t for a fixed $\bar{\mathbf{w}}_t$, and for any $(\mathbf{v}, b) \in \mathcal{V}$, $\mathcal{L}(\mathbf{v}, b)$ is called a *section* of \mathcal{L} at (\mathbf{v}, b) (see page 16 in [49]). Henceforth, we assume that $\tau_c, \tau_d > \alpha$ to simplify the analysis; however, the main results are valid even if this assumption is relaxed. Proposition 4 asserts that the posets \mathcal{V} , \mathcal{L} and $\mathcal{L}(\mathbf{v}, b)$ are lattices.

Proposition 4 *The sets \mathcal{V} , \mathcal{L} and $\mathcal{L}(\mathbf{v}, b)$ are lattices.*

The proof of Proposition 4 is provided in the Appendix.

Next, we present our main result, Theorem 1, which asserts the multimodularity of V_t , and the monotonicity of \mathbf{x}_t^* , with respect to \mathbf{y}_t . With a slight abuse of notation, let $\Delta_i f(\bar{\mathbf{w}}_t, \mathbf{a})$ denote both the forward and backward finite differences of a function $f(\bar{\mathbf{w}}_t, \mathbf{a})$ with respect to dimension i of \mathbf{a} . Specifically, for some $\epsilon > 0$, the forward difference of f is

$$\Delta_i f(\bar{\mathbf{w}}_t, \mathbf{a}) = f(\bar{\mathbf{w}}_t, \mathbf{a} + \epsilon \mathbf{e}_i) - f(\bar{\mathbf{w}}_t, \mathbf{a}),$$

and the backward difference is $f(\bar{\mathbf{w}}_t, \mathbf{a}) - f(\bar{\mathbf{w}}_t, \mathbf{a} - \epsilon \mathbf{e}_i)$, where \mathbf{e}_i is the i th unit vector. Similarly, let $\Delta_{i,j} f(\bar{\mathbf{w}}_t, \mathbf{a})$ be the second-order finite difference of $f(\bar{\mathbf{w}}_t, \mathbf{a})$, with respect to dimensions i and j of \mathbf{a} , defined by

$$\Delta_{i,j} f(\bar{\mathbf{w}}_t, \mathbf{a}) = \Delta_j (\Delta_i f(\bar{\mathbf{w}}_t, \mathbf{a})).$$

Theorem 1 *For each $t \in T$ and a fixed exogenous state $\bar{\mathbf{w}}_t$,*

(i) $V_t(\bar{\mathbf{w}}_t, \mathbf{y}_t)$ *is multimodular in $\mathbf{y}_t \in \mathcal{Y}$;*

(ii) $V_t(\bar{\mathbf{w}}_t, \mathbf{y}_t)$ *has increasing differences and is component-wise convex in $\mathbf{y}_t \in \mathcal{Y}$. That is,*

$$\begin{aligned} \Delta_{1,1} V_t(\bar{\mathbf{w}}_t, \mathbf{y}_t) &\geq \Delta_{1,2} V_t(\bar{\mathbf{w}}_t, \mathbf{y}_t) \geq 0, \\ \Delta_{2,2} V_t(\bar{\mathbf{w}}_t, \mathbf{y}_t) &\geq \Delta_{2,1} V_t(\bar{\mathbf{w}}_t, \mathbf{y}_t) \geq 0; \end{aligned}$$

(iii) $\mathbf{x}_t^* = (\mathbf{u}_t^*, q_t^*)$ *is monotone decreasing in $\mathbf{y}_t \in \mathcal{Y}$. Furthermore, if q_t is fixed, then*

$$\begin{aligned} -1 &\leq \Delta_1 u_t^{1*}(\bar{\mathbf{w}}_t, \mathbf{y}_t) \leq \Delta_2 u_t^{1*}(\bar{\mathbf{w}}_t, \mathbf{y}_t) \leq 0, \\ -1 &\leq \Delta_2 u_t^{2*}(\bar{\mathbf{w}}_t, \mathbf{y}_t) \leq \Delta_1 u_t^{2*}(\bar{\mathbf{w}}_t, \mathbf{y}_t) \leq 0. \end{aligned}$$

The proof of Theorem 1 is provided in the Appendix. The multimodularity asserted in Theorem 1 (i) directly implies result (ii), which is often called the *diagonal-dominance* property (cf. [37, 60]) in the inventory literature. Multimodular value functions imply that the storage levels at the load buses are economic substitutes of each other. Theorem 1 (ii) implies result (iii). The monotonicity result in part (iii) asserts that, when the storage levels are high, it is more profitable to discharge and sell excess energy to the grid, rather than procuring energy and storing it. However, more insightful is the fact that the optimal storage decisions exhibit bounded sensitivities, as seen in the two inequalities of part (iii). That is, for each bus, using the optimal policy, a unit increase in the amount of stored energy yields less than a unit decrease in optimal charge/discharge decision. Furthermore, this marginal decrease is more sensitive to a local increase in the storage level, as opposed to an increase in the storage level at the other bus. The bounded sensitivities property shows that it need not be optimal to fully charge, or fully discharge, the storage devices at each stage, even when $\tau_c, \tau_d > \alpha$. That is, the optimal storage policy is not necessarily of the so-called “bang-bang” type, which is optimal in single-storage models that assume batteries with fast-charging capabilities (cf. [20, 42]). Thus, the bounded sensitivities property is indicative of a stable operating regime for the network and highlights the economic benefit of sharing stored energy under line capacity constraints.

3.3 Behavior of the Optimal Operational Cost

Here, we examine the behavior of the optimal operational cost z_α . This examination is motivated by the operator’s desire to determine the appropriate storage capacity at each bus prior to making any operational decisions. This determination is further warranted by the significant costs associated with storage investment in distribution networks. The operator’s storage allocation problem is formulated as follows:

$$\min_{\alpha} \kappa \sum_{i \in C'} \alpha_i + z_\alpha, \quad (18a)$$

$$\text{s.t. } \mathbf{0} \leq \alpha \leq \bar{\alpha}, \quad (18b)$$

where κ is the per-unit cost of storage capacity, and $\bar{\alpha}$ is a budget vector of the maximum storage capacity allowed at each bus. Proposition 5 asserts that the optimal operational cost is convex and monotone decreasing in the storage capacities.

Proposition 5 *The optimal operational cost z_α is convex and monotone decreasing in α .*

The proof of the proposition is provided in the Appendix. This result implies that additional storage capacity leads to lower costs, but with decreasing marginal benefit.

Next, we compare the operational cost of the 2-bus network to those of two comparable networks having distinct storage configurations. The 2-bus network has a *coupled storage* (CS) configuration, in which the two buses can transmit stored energy between them. By contrast, energy cannot be transmitted between the buses in a *decentralized storage* (DS) setting; thus, there is no interaction

between the buses, and the operational cost is the sum of the operational costs incurred at each of the buses. Finally, a *pooled storage* (PS) configuration consists of a centralized storage facility that satisfies the collective energy demand in the network. Figure 2 depicts these three networks and their storage configurations. It is assumed that the total storage capacity in each network is equal to $\alpha_1 + \alpha_2$. Additionally, it is assumed that both the charging and the discharging efficiencies in each network are equal to ρ for a fixed $\rho \in (0, 1]$.

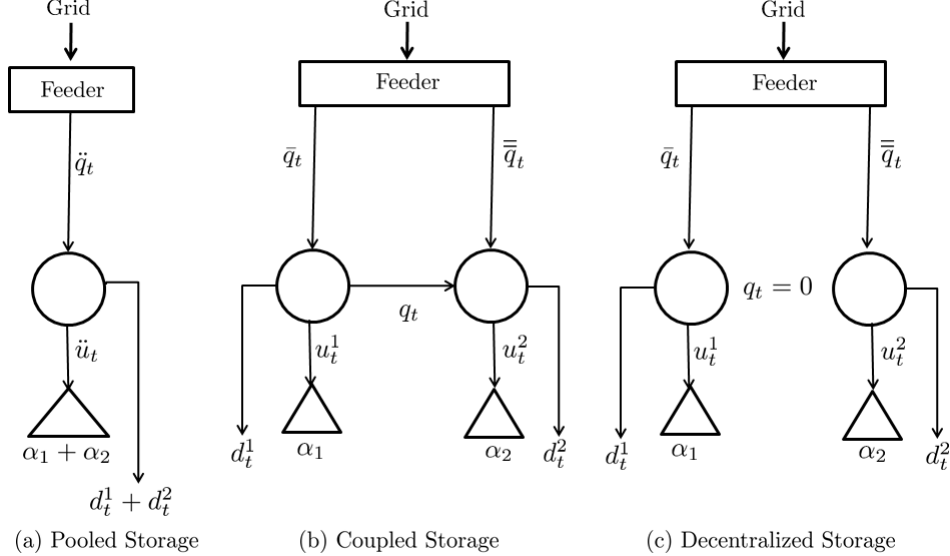


Figure 2: The pooled, coupled and decentralized storage configurations.

Theorem 2 asserts that the network with pooled storage has the lowest operational cost, followed by the one with coupled storage, which in turn is less than the cost in the decentralized storage network. For ease of exposition, let z_P , z_C and z_D denote the optimal operational costs of the PS, CS and DS network configurations, respectively. The next result shows how these costs compare to one another.

Theorem 2 *The optimal operational costs of PS, CS and DS configurations are ordered such that $z_P \leq z_C \leq z_D$.*

Proof. As $q_t = 0 \in [-\beta, \beta]$ at each stage $t \in T'$ in the DS network, it is clear that any optimal policy for the DSf network is a feasible, but not necessarily optimal, policy for the CS network; therefore, we have $z_C \leq z_D$. Next, we show that $z_P \leq z_C$. Assume that the initial storage levels in the CS and PS networks are zero without loss of generality. Let $\mathbf{u}_t^* = (u_t^{1*}, u_t^{2*})$ be the optimal charge/discharge decisions in the CS network at stage t . Construct a storage policy for the PS network, denoted by $\tilde{\pi} = (\tilde{u}_t : t \in T')$, such that $\tilde{u}_t = u_t^{1*} + u_t^{2*}$ for each $t \in T'$. Let \tilde{y}_t be the associated storage level realized at stage t under policy $\tilde{\pi}$, where $\tilde{y}_{t+1} = \tilde{y}_t + \tilde{u}_t$. Then, starting from $\tilde{y}_t = 0$, it is easy to verify that $0 \leq \tilde{y}_t + \tilde{u}_t \leq \alpha_1 + \alpha_2$ for each $t \in T'$, which implies that $\tilde{\pi}$ is

a feasible policy for the PS network. Next, define the variables $(\ddot{\theta}_t : t \in T')$, such that

$$\ddot{\theta}_t = \begin{cases} 1/\rho, & \ddot{u}_t \geq 0, \\ \rho, & \ddot{u}_t < 0. \end{cases}$$

Consider a realization $\mathbf{w} = (\mathbf{w}_t : t \in T)$ of the exogenous process \mathbf{W} . The one-step cost incurred at stage t in the PS network, when the state $(\mathbf{w}_t, \ddot{y}_t)$ is realized, is

$$\ddot{c}_t(\mathbf{w}_t, \ddot{u}_t) = p_t(d_t^1 + d_t^2 + \ddot{\theta}_t \ddot{u}_t) + \varphi|\ddot{u}_t|,$$

while the corresponding one-step cost in the CS network for state $(\mathbf{w}_t, \mathbf{q}_t^*)$ is

$$c_t(\mathbf{w}_t, \mathbf{u}_t^*, \mathbf{q}_t^*) = p_t(d_t^1 + d_t^2 + \theta_t^1 u_t^{1*} + \theta_t^2 u_t^{2*}) + \varphi(|u_t^{1*}| + |u_t^{2*}|) + \nu \xi(\mathbf{u}_t^*, \mathbf{q}_t^*).$$

Define $\ddot{a}_t \equiv \ddot{\theta}_t \ddot{u}_t$ and $a_t \equiv \theta_t^1 u_t^{1*} + \theta_t^2 u_t^{2*}$. Next, compare the terms $\ddot{c}_t(\mathbf{w}_t, \ddot{u}_t)$ and $c_t(\mathbf{w}_t, \mathbf{u}_t^*, \mathbf{q}_t^*)$. To this end, consider the following six cases involving u_t^{1*} , u_t^{2*} and $\ddot{u}_t \equiv u_t^{1*} + u_t^{2*}$:

Case 1: $u_t^{1*} \geq 0$, $u_t^{2*} \geq 0$ and $u_t^{1*} + u_t^{2*} \geq 0$. Then $\theta_t^1 = \theta_t^2 = \ddot{\theta}_t = 1/\rho$, and $a_t = \ddot{a}_t = (u_t^{1*} + u_t^{2*})/\rho$.

Case 2: $u_t^{1*} \geq 0$, $u_t^{2*} < 0$ and $u_t^{1*} + u_t^{2*} \geq 0$. Then $\theta_t^1 = \ddot{\theta}_t = 1/\rho$, $\theta_t^2 = \rho$, and $a_t = u_t^{1*}/\rho + \rho u_t^{2*} \geq (u_t^{1*} + u_t^{2*})/\rho = \ddot{a}_t$.

Case 3: $u_t^{1*} < 0$, $u_t^{2*} \geq 0$ and $u_t^{1*} + u_t^{2*} \geq 0$. Then $\theta_t^1 = \rho$, $\theta_t^2 = \ddot{\theta}_t = 1/\rho$, and $a_t = \rho u_t^{1*} + u_t^{2*}/\rho \geq (u_t^{1*} + u_t^{2*})/\rho = \ddot{a}_t$.

Case 4: $u_t^{1*} < 0$, $u_t^{2*} < 0$ and $u_t^{1*} + u_t^{2*} < 0$. Then $\theta_t^1 = \theta_t^2 = \ddot{\theta}_t = \rho$, and $a_t = \ddot{a}_t = \rho(u_t^{1*} + u_t^{2*})$.

Case 5: $u_t^{1*} < 0$, $u_t^{2*} \geq 0$ and $u_t^{1*} + u_t^{2*} < 0$. Then $\theta_t^1 = \ddot{\theta}_t = \rho$, $\theta_t^2 = 1/\rho$, and $a_t = \rho u_t^{1*} + u_t^{2*}/\rho \geq \rho(u_t^{1*} + u_t^{2*}) = \ddot{a}_t$.

Case 6: $u_t^{1*} \geq 0$, $u_t^{2*} < 0$ and $u_t^{1*} + u_t^{2*} < 0$. Then $\theta_t^1 = 1/\rho$, $\theta_t^2 = \ddot{\theta}_t = \rho$, and $a_t = u_t^{1*}/\rho + \rho u_t^{2*} \geq \rho(u_t^{1*} + u_t^{2*}) = \ddot{a}_t$.

Clearly, $a_t \geq \ddot{a}_t \Rightarrow \theta_t^1 u_t^{1*} + \theta_t^2 u_t^{2*} \geq \ddot{\theta}_t \ddot{u}_t$ in all of the above cases. Also, $|\ddot{u}_t| = |u_t^{1*} + u_t^{2*}| \leq |u_t^{1*}| + |u_t^{2*}|$ by the triangle inequality, and $\nu \xi(u_t^*, q_t^*) \geq 0$ by definition. Therefore, $c_t(\mathbf{w}_t, \mathbf{u}_t^*, \mathbf{q}_t^*) \geq \ddot{c}_t(\mathbf{w}_t, \ddot{u}_t)$ for each $t \in T'$. Adding the one-step costs over the decision stages and taking expectation of these sums, we obtain

$$\mathbb{E}_{\tilde{\pi}} \left(\sum_{t \in T'} \ddot{c}_t(\mathbf{w}_t, \ddot{u}_t) \right) \leq \mathbb{E}_{\pi^*} \left(\sum_{t \in T'} c_t(\mathbf{w}_t, \mathbf{u}_t^*, \mathbf{q}_t^*) \right) = z_C. \quad (19)$$

However, the l.h.s. of (19) is greater than or equal to z_P because $\tilde{\pi}$ is a feasible, but not necessarily optimal, policy for the PS network. This concludes the proof. \blacksquare

To the authors' knowledge, Theorem 2 is the first result to establish theoretical bounds on the optimal operational cost (z_C) incurred in a 2-bus distribution network with storage; however, the upper and lower bounds of z_C (z_D and z_P , respectively) need not be tight in general. Specifically, these bounds are the optimal costs of simplified, single-storage models that do not account for energy flow constraints in a 2-bus network. It is well-known that optimal storage policies for single-storage models exhibit a dual-threshold structure (cf. [20, 26, 43, 50, 53]), allowing such models

to be solved efficiently using specialized backward induction algorithms (see Section 4.7.6 in [40]). It is instructive that the quantity $z_C - z_P$ represents the cost savings achieved by pooling stored energy in a centralized facility, while the quantity $z_D - z_C$ can be interpreted as the opportunity cost of prohibiting the transmission of stored energy between the buses. Consequently, the ratio $(z_D - z_P)/z_D$ can be viewed as the marginal benefit of centralizing the storage operations of two decentralized storage systems.

3.4 Extension to Multi-bus Networks

In this subsection, we extend the results of Theorems 1 and 2 to networks with more than two buses. Specifically, we consider *loop* and *mesh* network configurations, which are common for distribution networks [13]. Figure 3 depicts these two configurations, which differ primarily in the number of line connections between the buses. The mesh configuration is a fully-connected network topology in which each pair of buses is connected by a line. By contrast, a loop network is a simply connected network. Let G denote the total number of load buses in the network, and let

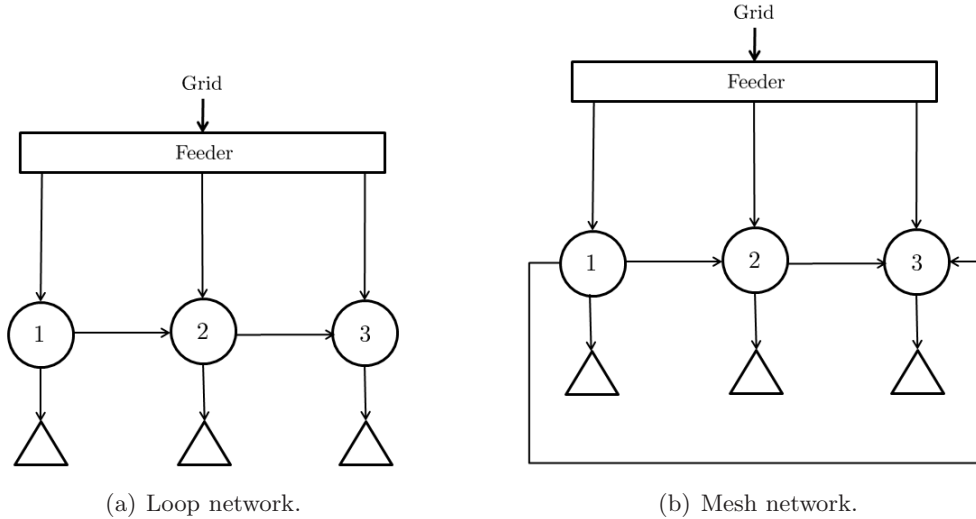


Figure 3: Depiction of networks with the loop and the mesh configurations.

$C' \equiv \{1, \dots, G\}$ denote the set of such buses. The set of lines in the loop and the mesh networks are denoted by A_L and A_M , respectively. For both networks, let \bar{q}_t^i be the energy flow in the feeder line connected to bus i , and let $q_t(i, j)$ denote the energy flow in line (i, j) , where $q_t(i, j) \geq 0$ if energy flows from bus i to bus j , and $q_t(i, j) < 0$ otherwise. For notational convenience, denote $q_t(G, G+1) \equiv q_t(G, 1)$. For each $t \in T'$ and $i \in C'$, the supply-demand balance constraints in these two multi-bus networks are

$$\begin{aligned}
 \text{(Loop)} \quad \bar{q}_t^i &= d_t^i + \theta_t^i u_t^i + q_t(i, i+1) - q_t(i-1, i), \\
 \text{(Mesh)} \quad \bar{q}_t^i &= d_t^i + \theta_t^i u_t^i + \sum_{(i,j) \in A_M: j > i} q_t(i, j) - \sum_{(j,i) \in A_M: j < i} q_t(j, i).
 \end{aligned}$$

Let $\mathbf{q}_t^L = (q_t(i, j) : (i, j) \in A_L)$ and $\mathbf{q}_t^M = (q_t(i, j) : (i, j) \in A_M)$ be the vector of energy flows between the load buses in the loop and the mesh networks, respectively. Then, one-step costs incurred at stage t in the two multi-bus networks are

$$\begin{aligned} \text{(Loop)} \quad c_t^L(\mathbf{s}_t, \mathbf{x}_t) &= p_t \sum_{i \in C'} (d_t^i + \theta_t^i u_t^i) + \varphi \sum_{i \in C'} |u_t^i| + \nu \xi(\mathbf{u}_t, \mathbf{q}_t^L), \\ \text{(Mesh)} \quad c_t^M(\mathbf{s}_t, \mathbf{x}_t) &= p_t \sum_{i \in C'} (d_t^i + \theta_t^i u_t^i) + \varphi \sum_{i \in C'} |u_t^i| + \nu \xi(\mathbf{u}_t, \mathbf{q}_t^M). \end{aligned}$$

The functions c_t^L and c_t^M are of the same form as that of c_t in (7). Moreover, the storage level and line capacity constraints in the multi-bus networks mirror those in the 2-bus network; hence, the lattice structure of the feasibility sets is conserved, despite the fact that the number of constraints is significantly higher for the multi-bus configurations. This leads us to the next result in Theorem 3 that holds for both the multi-bus networks and is stated without proof.

Theorem 3 *For each $t \in T$,*

- (i) $V_t(\bar{\mathbf{w}}_t, \mathbf{y}_t)$ is multimodular in $\mathbf{y}_t \in \mathcal{Y}$.
- (ii) \mathbf{x}_t^* is monotone decreasing in $\mathbf{y}_t \in \mathcal{Y}$.

The next result, Theorem 4, establishes a sequence of bounds involving the optimal costs of the pooled (z_P), decentralized (z_D), loop (z_L) and mesh (z_M) networks.

Theorem 4 *The optimal operational costs are ordered such that $z_P \leq z_M \leq z_L \leq z_D$.*

Proof. Note that, for the DS network, $q_t(i, j) = 0$ for all $(i, j) \in A_L$; therefore, it is clear that any optimal policy for the DS network is a feasible, but not necessarily optimal, policy for the loop network. Therefore, $z_L \leq z_D$. Similarly, $q_t(i, j) = 0$ for all $(i, j) \in A_M \setminus A_L$ in the loop network. Using a similar feasibility-optimality argument for the optimal costs of the loop and mesh networks, we conclude that $z_M \leq z_L$. Next, we show that $z_P \leq z_M$. Assume that the initial storage levels in the mesh and PS networks are zero without loss of generality. Let $\mathbf{u}_t^* = (u_t^{i*} : i \in C')$ be the optimal charge/discharge decisions in the mesh network at stage t . Construct a storage policy for the PS network, denoted by $\tilde{\boldsymbol{\pi}} = (\tilde{u}_t : t \in T')$, such that $\tilde{u}_t = \sum_{i \in C'} u_t^{i*}$ for each $t \in T'$. Let \tilde{y}_t be the storage level realized at stage t under policy $\tilde{\boldsymbol{\pi}}$, where $\tilde{y}_{t+1} = \tilde{y}_t + \tilde{u}_t$. Then, starting from $\tilde{y}_t = 0$, it is easy to verify that $0 \leq \tilde{y}_t + \tilde{u}_t \leq \sum_{i \in C'} \alpha_i$, which implies that $\tilde{\boldsymbol{\pi}}$ is a feasible policy for the PS network. Next, define the variables $(\tilde{\theta}_t : t \in T')$, such that

$$\tilde{\theta}_t = \begin{cases} 1/\rho, & \tilde{u}_t \geq 0, \\ \rho, & \tilde{u}_t < 0. \end{cases}$$

Next, we show that $\sum_{i \in C'} \theta_t^i u_t^{i*} \geq \tilde{\theta}_t \tilde{u}_t$ by using a simple induction argument. For $k \in C' \setminus \{1\}$, define $\tilde{u}_t^k \equiv \sum_{i=1}^k u_t^{i*}$, and let $\tilde{\theta}_t^k = 1/\rho$ if $\tilde{u}_t^k \geq 0$, and $\tilde{\theta}_t^k = \rho$ otherwise. From the proof of Theorem 2, we know that $\sum_{i=1}^k \theta_t^i u_t^{i*} \geq \tilde{\theta}_t^k \tilde{u}_t^k$ for $k = 2$. For the induction hypothesis, suppose $\sum_{i=1}^k \theta_t^i u_t^{i*} \geq \tilde{\theta}_t^k \tilde{u}_t^k$ for some $k > 2$. Adding the term $\theta_t^{k+1} u_t^{(k+1)*}$ to both sides, we obtain $\sum_{i=1}^{k+1} \theta_t^i u_t^{i*} \geq \tilde{\theta}_t^k \tilde{u}_t^k +$

$\theta_t^{k+1} u_t^{(k+1)*}$. Define $a_t \equiv \tilde{\theta}_t^k \tilde{u}_t^k + \theta_t^{k+1} u_t^{(k+1)*}$ and $\tilde{a}_t = \tilde{\theta}_t^{k+1} \tilde{u}_t^{k+1}$. Next, we compare the terms a_t and \tilde{a}_t for the following six cases involving the terms $\tilde{u}_t^k, \tilde{u}_t^{k+1}$ and $u_t^{(k+1)*}$:

Case 1: $\tilde{u}_t^k \geq 0$, $u_t^{(k+1)*} \geq 0$ and $\tilde{u}_t^{k+1} \geq 0$. Then $\tilde{\theta}_t^k = \tilde{\theta}_t^{k+1} = \theta_t^{(k+1)*} = 1/\rho$, and $a_t = \tilde{a}_t = \tilde{u}_t^{k+1}/\rho$.

Case 2: $\tilde{u}_t^k \geq 0$, $u_t^{(k+1)*} < 0$, and $\tilde{u}_t^{k+1} \geq 0$. Then $\tilde{\theta}_t^k = \tilde{\theta}_t^{k+1} = 1/\rho$, $\theta_t^{(k+1)*} = \rho$ and $a_t = \tilde{u}_t^k/\rho + \rho u_t^{(k+1)*} \geq \tilde{u}_t^{k+1}/\rho = \tilde{a}_t$.

Case 3: $\tilde{u}_t^k < 0$, $u_t^{(k+1)*} \geq 0$, and $\tilde{u}_t^{k+1} \geq 0$. Then $\tilde{\theta}_t^k = \rho$, $\theta_t^{(k+1)*} = \tilde{\theta}_t^{k+1} = 1/\rho$ and $a_t = \rho \tilde{u}_t^k + u_t^{(k+1)*}/\rho \geq \tilde{u}_t^{k+1}/\rho = \tilde{a}_t$.

Case 4: $\tilde{u}_t^k < 0$, $u_t^{(k+1)*} < 0$, and $\tilde{u}_t^{k+1} < 0$. Then $\tilde{\theta}_t^k = \theta_t^{(k+1)*} = \tilde{\theta}_t^{k+1} = \rho$ and $a_t = \tilde{a}_t = \rho \tilde{u}_t^{k+1}$.

Case 5: $\tilde{u}_t^k < 0$, $u_t^{(k+1)*} \geq 0$, and $\tilde{u}_t^{k+1} < 0$. Then $\tilde{\theta}_t^k = \tilde{\theta}_t^{k+1} = \rho$, $\theta_t^{(k+1)*} = 1/\rho$ and $a_t = \rho \tilde{u}_t^k + u_t^{(k+1)*}/\rho \geq \rho \tilde{u}_t^{k+1} = \tilde{a}_t$.

Case 6: $\tilde{u}_t^k \geq 0$, $u_t^{(k+1)*} < 0$, and $\tilde{u}_t^{k+1} < 0$. Then $\tilde{\theta}_t^k = 1/\rho$, $\theta_t^{(k+1)*} = \tilde{\theta}_t^{k+1} = \rho$ and $a_t = \tilde{u}_t^k/\rho + \rho u_t^{(k+1)*} \geq \rho \tilde{u}_t^{k+1} = \tilde{a}_t$.

Clearly, $a_t \geq \tilde{a}_t \Rightarrow \tilde{\theta}_t^k \tilde{u}_t^k + \theta_t^{k+1} u_t^{(k+1)*} \geq \tilde{\theta}_t^{k+1} \tilde{u}_t^{k+1}$. Finally, by the induction hypothesis, we obtain $\sum_{i=1}^{k+1} \theta_t^i u_t^{i*} \geq \tilde{\theta}_t^{k+1} \tilde{u}_t^{k+1}$, which proves that our induction hypothesis is true. For $k = M$, this is equivalent to $\sum_{i \in C'} \theta_t^i u_t^{i*} \geq \tilde{\theta}_t \tilde{u}_t$. The rest of the proof is similar to that of Theorem 2, from which we conclude that $z_D \leq z_M$. \blacksquare

4 Numerical Examples

In this section, we present numerical examples to illustrate the structural properties of the value function (V_t), the optimal policy (π^*) and the optimal operational cost (z_α) for a 2-bus network using real renewable generation and pricing data. Before presenting these examples, the source data, solution methodology and computational study are described in greater detail.

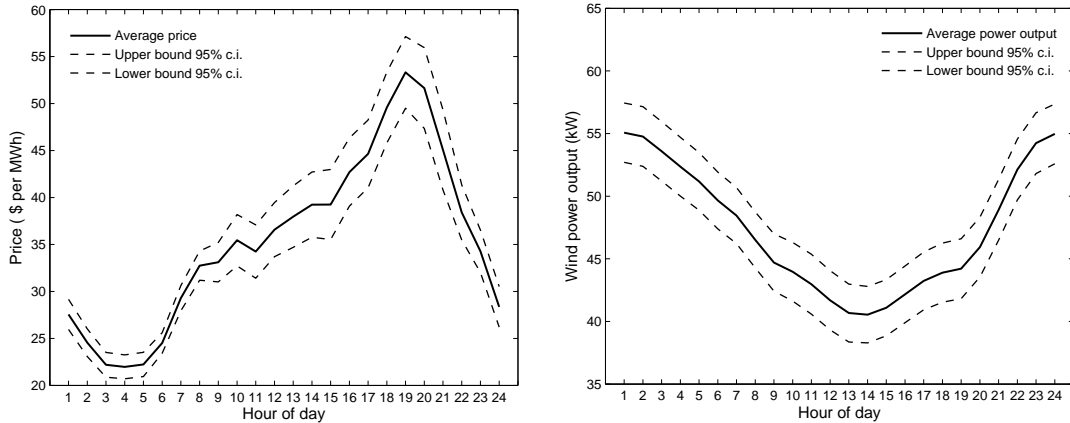
4.1 Data Description

Hourly wind speed and real-time electricity pricing data for calendar year 2012 were obtained from the NREL (National Renewable Energy Laboratory; <http://www.nrel.gov>) and PJM (Pennsylvania-Jersey-Maryland Interconnection; <http://www.pjm.com>), respectively. Let v_t and P_t be the wind speed and price in hour $t \in \{1, \dots, 24\}$, respectively. Due to seasonality effects, we partitioned both data sets into 24 segments, each one hour in duration, and fit separate probability density functions to each segment. The hourly prices were fit using truncated normal (TN) distributions of the form $P_t \sim TN(\hat{p}_t, \hat{\sigma}_t^2)$, where \hat{p}_t and $\hat{\sigma}_t^2$ are the (estimated) mean and variance of the price level in hour t , respectively. As was done in [14, 44], we fit the hourly wind speeds using Weibull distributions, i.e., $v_t \sim \text{Weibull}(\hat{\ell}_t, \hat{n}_t)$, where $\hat{\ell}_t$ and \hat{n}_t are the (estimated) shape and scale parameters, respectively. Each of the distribution parameters were estimated from the real data using maximum likelihood estimation (MLE), and the values are presented in Table 1. Next, we determined the wind generation levels at the two buses. Let R_t^i denote the wind generation in hour

t at bus i . It was assumed that the Evance R9000 wind turbine models is installed at both buses. The turbine at bus 1 has a power rating of $\bar{R}^1 = 50$ kW, while the turbine at bus 2 has a power rating of $\bar{R}^2 = 25$ kW. Both turbines have a cut-in speed of $v_c = 3$ meter per second (m/s), a cut-off speed of $v_f = 60$ m/s, and a rated wind speed of $\bar{v} = 12$ m/s. The following deterministic model (see p. 547 of [32]) was used to compute the hourly wind generation level at each bus i :

$$R_t^i = \begin{cases} \bar{R}^i \left(\frac{\bar{v} - v_t}{\bar{v} - v_c} \right), & v_c \leq v_t \leq \bar{v}, \\ \bar{R}^i, & \bar{v} \leq v_t \leq v_f, \\ 0, & \text{otherwise.} \end{cases}$$

For the analysis that follows, P_t, R_t^1 , and R_t^2 are assumed to be mutually independent random variables. Figure 4 depicts the average hourly wind generation at bus 1 and price levels (and associated 95% confidence intervals) for a 24-hour period. In this figure, hour 1 is midnight to 0100, hour 2 is 0100–0200, hour 3 is 0200–0300, and so forth. Examining Figure 4(a) closely, it is



(a) Real-time hourly electricity prices.

(b) Hourly wind generation levels at bus 1.

Figure 4: Average price and wind generation levels in the year 2012.

seen that the evening hours (hours 17 to 21) are the peak-price periods, while the off-peak price periods span the late night and early morning hours (hours 1 to 7). The variability in the hourly prices exhibits a similar trend. By contrast, as seen in Figure 4(b), wind power output is highest during the late night and early morning hours and is lowest in the afternoon (hours 12 to 16).

Next, we impose assumptions about the wind generation levels at the two buses. Let $\mathcal{R}_t^1, \mathcal{R}_t^2$ and \mathcal{P}_t denote the (bounded) supports of R_t^1, R_t^2 and P_t , respectively. The lower and upper limits of these sets correspond to their respective minimum and maximum values observed during 2012. In order to numerically compute the optimal policy, we assume finite supports for the exogenous variables. Theorem 6.10.11 of [40] provides an error bound for finite-state approximations to countable-state MDP models. These supports were therefore discretized as follows: $\mathcal{R}_t^1 = \mathcal{R}_t^2 = \{0, 1, \dots, 9\}$, and $\mathcal{P}_t = \{5n : n = 0, 1, \dots, 12\}$. Let ϕ_t, ϑ_t^1 and ϑ_t^2 be the probability density functions of P_t, R_t^1 and R_t^2 , respectively. For ease of computation, we fix the hourly demand levels at their mean values (obtained from PJM demand data). Therefore, the (random) exogenous state \mathbf{W}_t consists of the

Table 1: MLE estimates of the wind energy and price distribution parameters.

t	1	2	3	4	5	6	7	8	9	10	11	12
$\hat{\ell}_t$	4.51	4.49	4.41	4.36	4.33	4.29	4.22	4.08	3.81	3.61	3.56	3.59
\hat{n}_t	2.09	2.08	2.06	2.02	1.99	1.96	1.89	1.79	1.59	1.46	1.43	1.43
\hat{p}_t	27.26	25.65	23.48	23.39	23.75	25.65	28.47	32.46	33.67	36.82	34.95	37.64
$\hat{\sigma}_t^2$	6.50	9.45	10.42	12.91	14.56	15.18	15.43	18.21	19.36	21.59	20.07	24.31
t	13	14	15	16	17	18	19	20	21	22	23	24
$\hat{\ell}_t$	3.62	3.71	3.78	3.85	3.87	3.83	3.78	3.86	4.07	4.31	4.46	4.52
\hat{n}_t	1.43	1.44	1.67	1.49	1.50	1.52	1.55	1.59	1.72	1.87	1.98	2.03
\hat{p}_t	38.54	39.94	40.67	41.52	44.85	46.64	50.33	52.78	51.08	38.85	34.71	28.25
$\hat{\sigma}_t^2$	25.74	26.25	28.53	28.21	29.03	30.33	32.74	36.59	31.28	26.65	18.19	14.09

price and wind generation levels only, i.e., $\mathbf{W}_t = (P_t, R_t^1, R_t^2)$, so that $\mathcal{W}_t = \mathcal{P}_t \times \mathcal{R}_t^1 \times \mathcal{R}_t^2$. Let g_t be the joint probability mass function of \mathbf{W}_t . Then, due to the independence assumption, the exogenous process transitions from state $\mathbf{w}_{t-1} \in \mathcal{W}_{t-1}$ to another state $\mathbf{w}_t = (p, r_1, r_2) \in \mathcal{W}_t$ with probability

$$\mathbb{P}_{t-1}(\mathbf{w}_t | \mathbf{w}_{t-1}) = g_t(\mathbf{w}_t) = \frac{\phi_t(p)}{\sum_{\tilde{p} \in \mathcal{P}_t} \phi_t(\tilde{p})} \times \frac{\vartheta_t^1(r_1)}{\sum_{\tilde{r}_1 \in \mathcal{R}_t^1} \vartheta_t^1(\tilde{r}_1)} \times \frac{\vartheta_t^2(r_2)}{\sum_{\tilde{r}_2 \in \mathcal{R}_t^2} \vartheta_t^2(\tilde{r}_2)}. \quad (20)$$

For the problem instances that follow, we used the parameter values of Table 2. It was assumed that both buses have identical energy storage parameters $\alpha_i, \rho_c^i, \rho_d^i, \tau_c^i$ and τ_d^i . Moreover, the storage devices were assumed to have a shelf-life exceeding one year.

Table 2: Summary of parameter values for the problem instances.

Parameter(s)	Parameter descriptions	Value(s)
(α_1, α_2)	Storage capacities at buses 1 and 2 (in kW-h)	(10,10)
(τ_c^i, τ_d^i)	Storage charging and discharging rates at buses 1 and 2 (in kW)	(4,4)
(ρ_c^i, ρ_d^i)	Storage charging and discharging efficiencies at buses 1 and 2	(0.90,0.85)
β	Line capacity (in kW-h)	3.5
φ	Per-unit cost of charging or discharging energy (dollars/kW-h)	10
ν	Per-unit cost of line losses (dollars/kW-h)	20

The parameter φ can be viewed as the implicit cost of degradation per unit of energy charged or discharged from the battery and can be determined using a life-cycle cost analysis that accounts for several factors affecting battery performance, such as temperature, state-of-charge profile, and depth-of-discharge limits (see [5, 21, 22]). Similarly, the quantity ν can be estimated by using a life-cycle cost model (e.g., equation (6) of [57]), which uses the resistance per unit length of the power lines, per unit electricity prices, and the maximum allowable current in the power lines.

4.2 Solving the MDP Model

For the computational experiments, we considered a 24-hour (or 25-stage) planning horizon, i.e., $T = \{1, \dots, 25\}$, in January 2012. It is assumed that decisions are made at the start of each hour (or stage). Moreover, the state space in each stage was assumed to be time invariant, i.e., $\mathcal{S}_t = \mathcal{S}$ for all $t \in T$. We discretized the storage levels, Y_t^1 and Y_t^2 , to have support $\mathcal{Y} = \{0, 1, \dots, 10\} \times \{0, 1, \dots, 10\}$. Hence, there are $13 \times 10^2 \times 11^2 = 157,300$ possible states in each stage.

We employ the linear programming (LP) approach devised in [8] to solve the non-stationary, finite-horizon model (8) and begin by introducing its primal LP formulation. For notational convenience, denote $\mathcal{X}_t(\mathbf{s})$ simply as \mathcal{X}_t . Let $(\lambda_t(\mathbf{s}) : t \in T', \mathbf{s} \in \mathcal{S})$ be the vector of primal LP variables, and $(\gamma_t(\mathbf{s}) : t \in T', \mathbf{s} \in \mathcal{S})$ be the vector of cost coefficients such that $\gamma_t(\mathbf{s}) \in (0, \infty)$ for each $t \in T'$ and $\mathbf{s} \in \mathcal{S}$. The primal LP formulation is

$$\max \sum_{t \in T'} \sum_{\mathbf{s} \in \mathcal{S}} \gamma_t(\mathbf{s}) \lambda_t(\mathbf{s}) \quad (21a)$$

$$\text{s.t. } \lambda_t(\mathbf{s}) \leq c_t(\mathbf{s}, \mathbf{x}) + \delta \sum_{\mathbf{s}' \in \mathcal{S}} \mathbb{P}_t(\mathbf{s}' | \mathbf{s}, \mathbf{x}) \lambda_{t+1}(\mathbf{s}'), \quad \forall t \in T', \mathbf{s} \in \mathcal{S}, \mathbf{x} \in \mathcal{X}_t, \quad (21b)$$

$$\lambda_t(\mathbf{s}) \in \mathbb{R}. \quad (21c)$$

Let $(\lambda_t^*(\mathbf{s}) : t \in T', \mathbf{s} \in \mathcal{S})$ be the vector of optimal solutions of (21). As $\gamma_t(\mathbf{s}) > 0$, it must be the case that the constraints (21b) hold with equality at optimality, i.e.,

$$\lambda_t^*(\mathbf{s}) = c_t(\mathbf{s}, \mathbf{x}) + \delta \sum_{\mathbf{s}' \in \mathcal{S}} \mathbb{P}_t(\mathbf{s}' | \mathbf{s}, \mathbf{x}) \lambda_{t+1}^*(\mathbf{s}'), \quad \forall t \in T', \mathbf{s} \in \mathcal{S}, \mathbf{x} \in \mathcal{X}_t,$$

which implies that $\lambda_t^*(\mathbf{s}) = V_t(\mathbf{s})$ by Bellman's optimality principle. Thus, we can recover the value functions of (8) by solving model (21). Note if we choose $\gamma_1(\mathbf{s}) = \mathbb{P}(\mathbf{S}_1 = \mathbf{s})$, such that $\sum_{\mathbf{s} \in \mathcal{S}} \gamma_1(\mathbf{s}) = 1$, we can express the optimal value of (8) according to

$$z_\alpha = \sum_{\mathbf{s} \in \mathcal{S}} \gamma_1(\mathbf{s}) \lambda_1^*(\mathbf{s}) = \sum_{\mathbf{s} \in \mathcal{S}} \gamma_1(\mathbf{s}) V_1(\mathbf{s}).$$

Unfortunately, the number of constraints in formulation (21) is prohibitively large for the problem instances considered in our numerical examples; hence, we solve the dual of (21), which has significantly fewer constraints. Let $(\mu_t(\mathbf{s}, \mathbf{x}) : t \in T', \mathbf{s} \in \mathcal{S}, \mathbf{x} \in \mathcal{X}_t)$ be the vector of dual variables associated with constraints (21b). Define $T'' \equiv \{1, \dots, N-2\}$. Then, the dual of problem (8) is

$$\min \sum_{t \in T'} \sum_{\mathbf{s} \in \mathcal{S}} \sum_{\mathbf{x} \in \mathcal{X}_t} c_t(\mathbf{s}, \mathbf{x}) \mu_t(\mathbf{s}, \mathbf{x}) \quad (22a)$$

$$\text{s.t. } \sum_{\mathbf{x} \in \mathcal{X}_1} \mu_1(\mathbf{s}, \mathbf{x}) = \gamma_1(\mathbf{s}), \quad \forall \mathbf{s} \in \mathcal{S}, \quad (22b)$$

$$\sum_{\mathbf{x} \in \mathcal{X}_t} \mu_{t+1}(\mathbf{s}, \mathbf{x}) - \delta \sum_{\mathbf{s}' \in \mathcal{S}} \sum_{\mathbf{x} \in \mathcal{X}_t} \mathbb{P}_t(\mathbf{s} | \mathbf{s}', \mathbf{x}) \mu_t(\mathbf{s}', \mathbf{x}) = \gamma_{t+1}(\mathbf{s}), \quad \forall t \in T'', \mathbf{s} \in \mathcal{S}, \quad (22c)$$

$$\mu_t(\mathbf{s}, \mathbf{x}) \geq 0, \quad \forall t \in T', \mathbf{s} \in \mathcal{S}, \mathbf{x} \in \mathcal{X}_t. \quad (22d)$$

It can be shown that the optimal solution of (22) has a one-to-one correspondence with the optimal policy of (8). That is, for each $\mathbf{s} \in \mathcal{S}_t$, $\mu_t^*(\mathbf{s}, \mathbf{x}) > 0$ when $\mathbf{x} = \mathbf{x}_t^*$, and $\mu_t^*(\mathbf{s}, \mathbf{x}) = 0$ otherwise (see the discussion in [8]). Therefore, the optimal policy $\boldsymbol{\pi}^*$ can be recovered directly from the optimal solution of model (22). The model was coded in Python 2.7 and solved using Gurobi 6.5. The discount factor δ was set to 0.99. All problem instances were executed on a Windows-based 64-bit, 4th generation, Intel[®] Core[™] i7, 64 GB, 2.9 GHz Windows machine.

4.3 Results and Discussion

First, we illustrate the behavior of the value functions with respect to the storage levels. For a given storage level vector \mathbf{y}_t , the *average value function*, denoted by $\bar{V}_t(\mathbf{y}_t)$, is

$$\bar{V}_t(\mathbf{y}_t) = \sum_{\mathbf{w}_t \in \mathcal{W}_t} \mathbb{P}(\mathbf{W}_t = \mathbf{w}_t) V_t(\mathbf{w}_t, \mathbf{y}_t), \quad \mathbf{y}_t \in \mathcal{Y}.$$

Figure 5 depicts the average value functions at stages 1 and 17 as functions of the storage levels. Clearly, $\bar{V}_t(\mathbf{y}_t)$ is monotone decreasing and convex in \mathbf{y}_t . This implies that the expected future cost decreases with increasing storage levels but with decreasing marginal benefit. Similar trends were observed at all other stages in the planning horizon. Interestingly, the surface plot in Figure 5(b) has a steeper slope than the one in Figure 5(a), particularly at lower storage levels. This is because

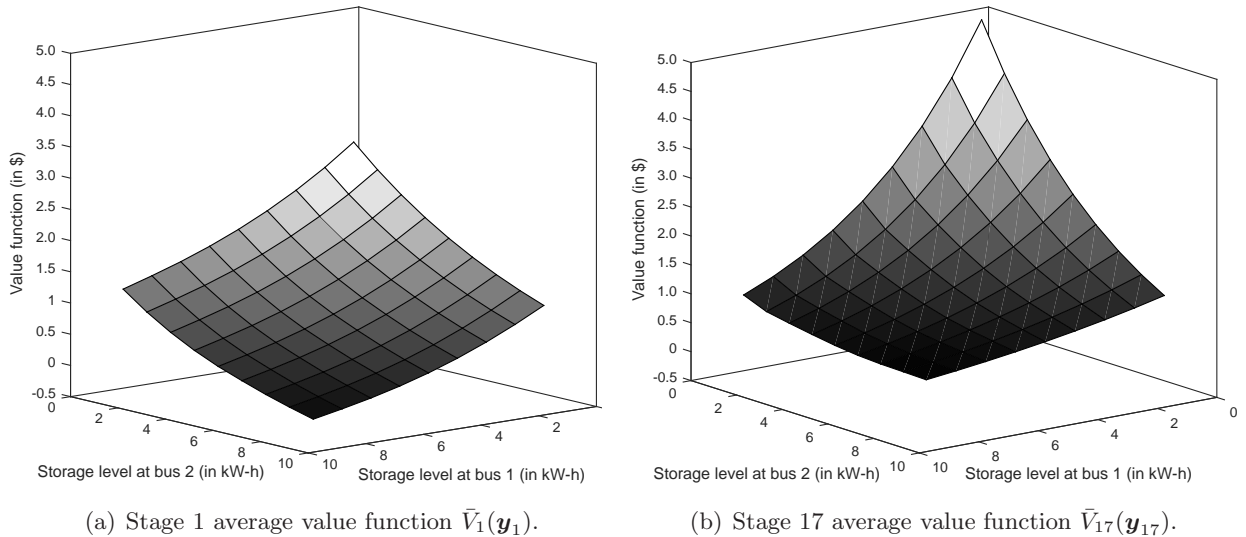


Figure 5: Average value functions $\bar{V}_t(\mathbf{y}_t)$ in stages 1 and 17.

stage 17 marks the onset of the peak-price periods – characterized by high price variability – in which procurement costs rise rapidly when stored energy is in short supply. Note that the average value of the function $\bar{V}_1(\mathbf{y}_1)$ over its domain \mathcal{Y} represents the daily, optimal operational cost of using a storage system with total capacity $\bar{\alpha} = \alpha_1 + \alpha_2$. Then, the marginal benefit (or marginal value) of using storage can be defined as the difference between the operational costs at capacities 0 and $\bar{\alpha}$. For instance, the marginal benefit of using storage was equal to \$26.75 for the problem instance used here ($\bar{\alpha} = 20$ kW-h).

Next, to illustrate the main results of Theorem 1, Figure 6 depicts the optimal charge/discharge decisions in stage $t = 17$ as functions of the storage levels for a fixed exogenous state. We note that the optimal storage decisions are monotone decreasing in the storage levels. Moreover, the optimal storage decision at each bus exhibits greater sensitivity to a marginal change in the storage level at that bus, as opposed to the storage level at the other bus. To illustrate this point, when y_2 is fixed at 10 kW-h, and y_1 increases from 0 to 10 kW-h, the optimal charge/discharge decision (u_t^{1*}) decreases from +2.97 kW-h to -3.03 kW-h as (i.e., $\Delta_1 u_t^{1*} = -0.6$). On the other hand, when y_1 is fixed at 10 kW-h, and y_2 increases from 0 to 10 kW-h, u_t^{1*} decreases from -2.95 kW-h to -3.32 kW-h (i.e., $\Delta_2 u_t^{1*} = -0.037$). Similar trends were observed in u_t^{2*} , and more generally, for all of the storage decisions at each stage $t \in T'$.

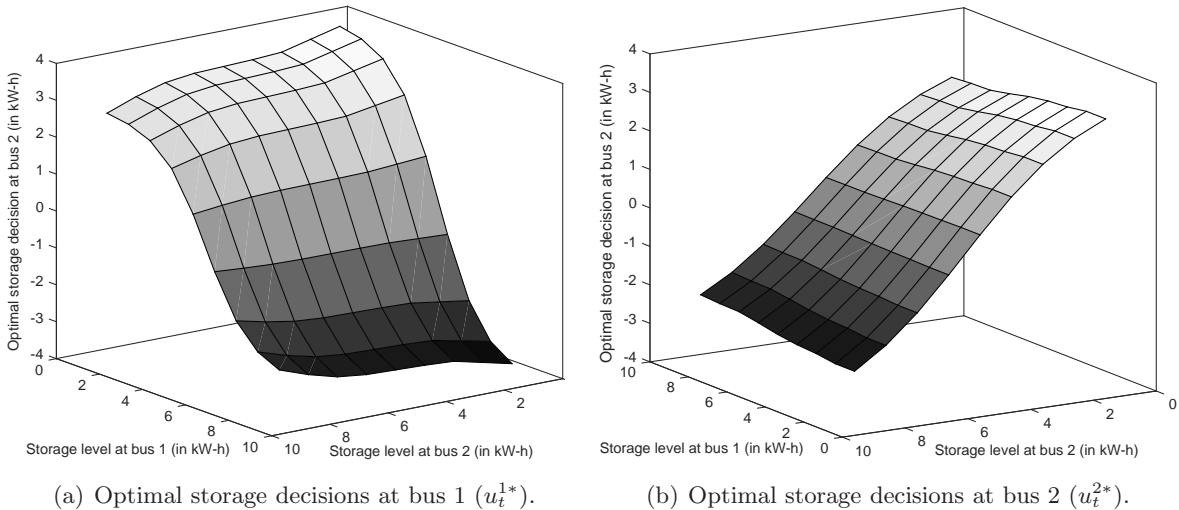


Figure 6: Optimal storage decisions in stage $t = 17$ when $\mathbf{w}_{17} = (30, 4.5, 4.5)$.

Finally, we compared the operational costs of the pooled storage (PS), 2-bus storage (CS), and decentralized storage (DS) networks for different storage capacities. For the sake of comparison, we fixed $\alpha_2 = 10$ kW-h and varied α_1 from 1 to 15 kW-h in intervals of 1 kW-h. Figure 7 depicts the relative magnitudes of the optimal operational costs of the three network configurations as functions of α_1 , illustrating Theorem 2. As the optimal policies of single-storage models exhibit a dual-threshold structure [20, 50], the pooled and the decentralized storage models were solved using the monotone value iteration algorithm (see [40]). It is evident from Figure 7 that, for all three networks, the operational cost decreases with increasing storage capacity but with decreasing marginal benefit. Moreover, the differences between the operational costs of each decreases rapidly as the storage capacity at bus 1 increases. This behavior stems from the increased flexibility of using stored energy to satisfy demand locally at each bus without having to transmit much energy between them. Although Theorem 2 establishes the relative magnitudes of these operational costs, it is clear from Figure 7 that the bounds are not tight, especially at low storage capacities.

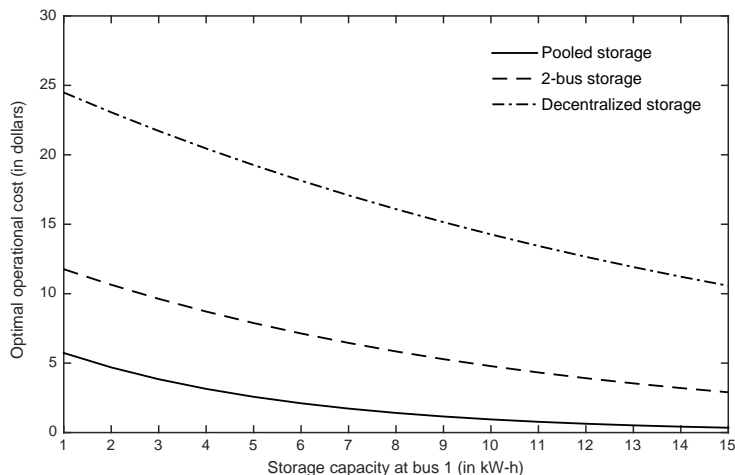


Figure 7: Comparison of the optimal operational costs in PS, CS, and DS networks.

This is indicative of non-negligible line-loss costs in energy networks with capacitated lines and storage systems. Hence, optimal policies derived from single-storage models are not suitable for distribution networks, as they do not adequately capture interactions between distinct storage devices in a networked environment.

5 Conclusions

We have examined optimal energy storage and flow strategies in a 2-bus distribution network with storage devices and line losses. The network operator’s objective is to minimize the total expected discounted costs incurred over a finite planning horizon by optimally selecting the amount of energy to charge to, or discharge from, the storage devices, the amount of energy to buy from, or sell to, the grid and the amount of energy to transmit between the buses. By way of a finite-horizon, discounted cost MDP model, we established the monotonicity of the optimal policy with respect to the storage levels. Moreover, we proved the multimodularity of the value function in the storage levels and that the optimal storage decisions at each stage exhibit bounded sensitivities. Significantly, we also established bounds that compare the cost of the 2-bus network to the costs of two comparable networks with pooled and decentralized storage configurations, respectively. The results of the 2-bus network were extended to more general multi-bus network topologies. The usefulness of the main results was illustrated by way of a numerical example using real pricing and wind generation data. Our results highlighted the benefits of using the network model over those of single-storage models that do not account for interactions between buses in a distribution network.

While the model and main structural results are useful, they can be improved in a few important ways. First, it is important to note that the structural results were established without accounting for reactive power flow and voltage level constraints in distribution networks. It will be necessary to examine more rigorous power-flow models (cf. [9, 54]) and extend our results to more realistic distribution networks. Second, it will be instructive to examine models that consider

multiple value-adding uses of storage (e.g., arbitrage, ancillary support, or backup energy). Third, it will be instructive to develop easily computable, tighter bounds for the optimal operational cost, similar to those established in Theorem 2.

Acknowledgments The authors are grateful to two anonymous referees, and the editors, for their constructive comments. This research was supported, in part, by grants from the Mascaro Center for Sustainable Innovation and the Center for Industry Studies (CIS) at the University of Pittsburgh.

References

- [1] U.S. Energy Information Administration. Annual energy outlook 2013. Technical report, U.S. Department of Energy, 2013.
- [2] K.H. Ahlert and C. van Dinther. Sensitivity analysis of the economic benefits from electricity storage at the end consumer level. In *Proceedings of the IEEE PowerTech Conference*, pages 1–8, 2009.
- [3] E. Altman, B. Gaujal, and A. Hordijk. Multimodularity, convexity, and optimization properties. *Mathematics of Operations Research*, 25(2):324–347, 2000.
- [4] O. Ardakanian, S. Keshav, and C. Rosenberg. *Integration of renewable generation and elastic loads into distribution grids*. Springer International, 2016.
- [5] M.O. Badawy, F. Cingoz, and Y. Sozer. Battery storage sizing for a grid tied PV system based on operating cost minimization. In *IEEE Energy Conversion Congress and Exposition (ECCE)*, pages 1–7, 2016.
- [6] A. Bar-Noy, Y. Feng, M. Johnson, and O. Liu. When to reap and when to sow: Lowering peak usage with realistic batteries. In *Lecture Notes in Computer Science*, volume 5038. Springer, 2008.
- [7] A. Bar-Noy, M. Johnson, and O. Liu. Peak shaving through resource buffering. In *Approximation and Online Algorithms*, volume 5426, pages 147–159. Springer, 2009.
- [8] A. Bhattacharya and J.P. Kharoufeh. Linear programming formulations for non-stationary, finite-horizon Markov decision process models. *Operations Research Letters*, 45(6):570–574, 2017.
- [9] A. Bhattacharya, J.P. Kharoufeh, and B. Zeng. Managing energy storage in microgrids: A multistage stochastic programming approach. *IEEE Transactions on Smart Grid*, 9(1):483–496, 2018.

- [10] E. Bitar, R. Rajagopal, P. Khargonekar, and K. Poolla. The role of co-located storage for wind power producers in conventional electricity markets. In *Proceedings of the American Control Conference*, pages 3886–3891, 2011.
- [11] S. Boyd and L. Vandenberghe. *Convex Optimization*. Cambridge University Press, 2004.
- [12] C. Brunetto and G. Tina. Optimal hydrogen storage sizing for wind power plants in day ahead electricity market. *IET Renewable Power Generation*, 1(4):220–226, 2007.
- [13] J. Casazza and F. Delea. *Understanding Electric Power Systems: An Overview of the Technology, the Marketplace, and Government Regulation, 2nd Edition*. John Wiley & Sons, 2010.
- [14] A.N. Celik. Energy output estimation for small-scale wind power generators using Weibull-representative wind data. *Journal of Wind Engineering and Industrial Aerodynamics*, 91(5):693–707, 2003.
- [15] J.J. Conti, P.D. Holtberg, J.A. Beamon, A.M. Schaal, G.E. Sweetnam, and A.S. Kydes. Annual Energy Outlook 2009: With Projections to 2030. Technical report, U.S. Energy Information Administration, 2009.
- [16] S. E. Dreyfus. An analytic solution of the warehouse problem. *Management Science*, 4(1):99–104, 1957.
- [17] J.M. Eyer, J.J. Iannucci, and G.P. Corey. Energy storage benefits and market analysis handbook, a study for the DOE energy storage systems program. Technical report, Sandia National Laboratories, 2004.
- [18] J.G. Gonzalez, R.M. de la Muela, L. M. Santos, and A.M. González. Stochastic joint optimization of wind generation and pumped-storage units in an electricity market. *IEEE Transactions on Power Systems*, 23(2):460–468, 2008.
- [19] B. Hajek. Extremal splittings of point processes. *Mathematics of Operations Research*, 10(4):543–556, 1985.
- [20] P. Harsha and M. Dahleh. Optimal management and sizing of energy storage under dynamic pricing for the efficient integration of renewable energy. *IEEE Transactions on Power Systems*, 30(3):1164–1181, 2015.
- [21] A. Hoke, A. Brissette, S. Chandler, A. Pratt, and D. Maksimović. Look-ahead economic dispatch of microgrids with energy storage, using linear programming. In *1st IEEE Conference on Technologies for Sustainability (SusTech)*, pages 154–161, 2013.
- [22] A. Hoke, A. Brissette, K. Smith, A. Pratt, and D. Maksimović. Accounting for lithium-ion battery degradation in electric vehicle charging optimization. *IEEE Journal of Emerging and Selected Topics in Power Electronics*, 2(3):691–700, 2014.

- [23] W. Hu, Z. Chen, and B. Bak-Jensen. Optimal operation strategy of battery energy storage system to real-time electricity price in Denmark. In *Proceedings of the IEEE Power and Energy Society General Meeting*, pages 1–7, 2010.
- [24] J.K. Kaldellis and D. Zafirakis. Optimum energy storage techniques for the improvement of renewable energy sources-based electricity generation and economic efficiency. *Energy*, 32(12):2295–2305, 2007.
- [25] S. Kaplan. Power plants: Characteristics and costs. Technical Report RL34746, Congressional Research Service, 2008.
- [26] J.H. Kim and W.B. Powell. Optimal energy commitments with storage and intermittent supply. *Operations Research*, 59(6):1347–1360, 2011.
- [27] M. Korpass, A.T. Holen, and R. Hildrum. Operation and sizing of energy storage for wind power plants in a market system. *International Journal of Electrical Power and Energy Systems*, 25(8):599–606, 2003.
- [28] I. Koutsopoulos, V. Hatzi, and L. Tassiulas. Optimal energy storage control policies for the smart power grid. In *IEEE International Conference on Smart Grid Communications*, pages 475–480, 2011.
- [29] R. Lasseter. Microgrids and distributed generation. *Journal of Energy Engineering*, 133(3):144–149, 2007.
- [30] D. Lee, J. Kim, and R. Baldick. Stochastic optimal control of the storage system to limit ramp rates of wind power output. *IEEE Transactions on Smart Grid*, 4(4):2256–2265, 2013.
- [31] Q. Li and P. Yu. Multimodularity and its applications in three stochastic dynamic inventory problems. *Manufacturing and Service Operations Management*, 16(3):455–463, 2014.
- [32] L. Lu. Stand-alone wind power and hybrid solar-wind power. In *Handbook of Clean Energy Systems*, volume 1, chapter 30. John Wiley & Sons, 2015.
- [33] P. Milgrom and C. Shannon. Monotone comparative statics. *Econometrica*, 62(1):157–180, 1994.
- [34] P. Mokrian and M. Stephen. A stochastic programming framework for the valuation of electricity storage. In *Proceedings of the 26th USAEE/IAEE North American Conference*, pages 24–27. IAEE, 2006.
- [35] J. Momoh. *Smart Grid: Fundamentals of Design and Analysis*. John Wiley & Sons, Inc., New York, NY, 2012.
- [36] B. Moradzadeh and K. Tomsovic. Two-stage residential energy management considering network operational constraints. *IEEE Transactions on Smart Grid*, 4(4):2339–2346, 2013.

- [37] K. Murota. Note on multimodularity and L-convexity. *Mathematics of Operations Research*, 30(3):658–661, 2005.
- [38] H. Oh. Aggregation of buses for a network reduction. *IEEE Transactions on Power Systems*, 27(2):705–712, 2012.
- [39] W.B. Powell. *Approximate Dynamic Programming: Solving the Curses of Dimensionality, 2nd Edition*. John Wiley & Sons, 2011.
- [40] M. L. Puterman. *Markov Decision Processes: Discrete Stochastic Dynamic Programming*. John Wiley & Sons, 2009.
- [41] S. Rao and D. Tylavsky. Nonlinear network reduction for distribution networks using the holomorphic embedding method. In *North American Power Symposium (NAPS)*, pages 1–6, 2016.
- [42] N. Secomandi. Optimal commodity trading with a capacitated storage asset. *Management Science*, 56(3):449–467, 2010.
- [43] N. Secomandi. Merchant commodity storage practice revisited. *Operations Research*., 63(5):1131–1143, 2015.
- [44] J. V. Seguro and T. W. Lambert. Modern estimation of the parameters of the Weibull wind speed distribution for wind energy analysis. *Journal of Wind Engineering and Industrial Aerodynamics*, 85(1):75–84, 2000.
- [45] D. Simchi-Levi, X. Chen, and J. Bramel. *Convexity and Supermodularity*, pages 15–44. Springer New York, 2014.
- [46] R. Sioshansi, P. Denholm, T. Jenkin, and J. Weiss. Estimating the value of electricity storage in PJM: Arbitrage and some welfare effects. *Energy Economics*, 31(2):269–277, 2009.
- [47] P. Sülc, S. Backhaus, and M. Chertkov. Optimal distributed control of reactive power via the alternating direction method of multipliers. *IEEE Transactions on Energy Conversion*, 29(4):968–977, 2014.
- [48] S. Suryanarayanan, F.M. David, J. Mitra, and Y. Li. Achieving the smart grid through customer-driven microgrids supported by energy storage. In *Proceedings of the IEEE International Conference on Industrial Technology (ICIT)*, pages 884–890, 2010.
- [49] D. M. Topkis. *Supermodularity and Complementarity*. Princeton University Press, Princeton, NJ, 1998.
- [50] P.M. Van de Ven, N. Hegde, L. Massoulié, and T. Salondis. Optimal control of end-user energy storage. *IEEE Transactions on Smart Grid*, 4(2):789–797, 2013.

- [51] N.S. Wade, P.C. Taylor, P.D. Lang, and P.R. Jones. Evaluating the benefits of an electrical energy storage system in a future smart grid. *Energy Policy*, 38(11):7180–7188, 2010.
- [52] J.B. Ward. Equivalent circuits for power-flow studies. *Transactions of the American Institute of Electrical Engineers*, 68(1):373–382, 1949i.
- [53] X. Xi, R. Sioshansi, and V. Marano. A stochastic dynamic programming model for co-optimization of distributed energy storage. *Energy Systems*, 5(3):475–505, 2014.
- [54] W. Yuan, J. Wang, F. Qiu, C. Chen, C. Kang, and B. Zeng. Robust optimization-based resilient distribution network planning against natural disasters. *IEEE Transactions on Smart Grid*, 7(6):2817–2826, 2016.
- [55] Y. Zhang, N. Gatsis, and G. B. Giannakis. Robust energy management for microgrids with high-penetration renewables. *IEEE Transactions on Sustainable Energy*, 4(4):944–953, 2013.
- [56] Y. Zhou, A. Scheller-Wolf, N. Secomandi, and S.F. Smith. Managing wind-based electricity generation in the presence of storage and transmission capacity. *Working Paper, Carnegie Mellon University*, 2014.
- [57] Z. Zhu, S. Lu, B. Gao, T. Yi, and B. Chen. Life cycle cost analysis of three types of power lines in 10 kV distribution network. *Inventions*, 1(4):71–80, 2016.
- [58] W. Zhuang and M.Z.F. Li. Monotone optimal control for a class of Markov decision processes. *European Journal of Operations Research*, 217(2):342–350, 2012.
- [59] P. H. Zipkin. *Foundations of Inventory Management*. McGraw-Hill, 2000.
- [60] P. H. Zipkin. On the structure of lost-sales inventory models. *Operations Research*, 56(4):937–944, 2008.

Appendix

Proof of Proposition 4

Proof. We first consider the set \mathcal{L} that is characterized by the following constraints:

$$0 \leq r_1 - b \leq \alpha_1, \quad (23a)$$

$$0 \leq r_2 - v_1 \leq \alpha_2, \quad (23b)$$

$$-\beta \leq r_3 - r_2 \leq \beta, \quad (23c)$$

$$0 \leq v_1 - b \leq \alpha_1, \quad (23d)$$

$$0 \leq v_2 - v_1 \leq \alpha_2. \quad (23e)$$

Define $\mathbf{a} \equiv (v, b, r) \in \mathcal{L}$. It is noted that each constraint in \mathcal{L} has exactly two variables with the coefficients $+1$ and -1 , while the remaining coefficients are equal to zero. Thus, each constraint in \mathcal{L} defines an affine half-space of the form $A_{i,j} = \{\mathbf{a} \in \mathbb{R}^6 : a_i - a_j \leq h, a_k = 0, i \neq j, k \neq i, j\}$. We show that each such $A_{i,j}$ is a lattice. Consider two points $\mathbf{a}, \mathbf{a}' \in A_{i,j}$. For the cases $\mathbf{a} \leq \mathbf{a}'$ and $\mathbf{a}' \leq \mathbf{a}$, it is easy to verify that $\mathbf{a} \vee \mathbf{a}' \in A_{i,j}$ and $\mathbf{a} \wedge \mathbf{a}' \in A_{i,j}$. Next, consider the case when $a_i \geq a'_i, a'_j \geq a_j$, and $a_k = a'_k = 0$ for all $k \neq i, j$. Then, the i th and j th components of $\mathbf{a} \wedge \mathbf{a}'$ and $\mathbf{a} \vee \mathbf{a}'$ are (a'_i, a_j) and (a_i, a'_j) , respectively. As $\mathbf{a} \in A_{i,j}$, $a_i \leq a_j + h$. But $a'_i \leq a_i$, and therefore, $a'_i \leq a_j + h \Rightarrow a'_i - a_j \leq h$, which implies that $\mathbf{a} \wedge \mathbf{a}' \in A_{i,j}$. Similarly, $a_i \leq h + a_j \leq h + a'_j \Rightarrow a_i - a'_j \leq h$ as $\mathbf{a}' \in A_{i,j}$ and $a'_j \geq a_j$, and therefore, $\mathbf{a} \vee \mathbf{a}' \in A_{i,j}$. Similar arguments are valid when $a_i \leq a'_i, a'_j \leq a_j$ and $a_k = a'_k = 0$ for all $k \neq i, j$; therefore, $A_{i,j}$ is a lattice. As a finite intersection of lattices is also a lattice (see Lemma 2.2.2 of [49]), \mathcal{L} is a lattice. Following similar lines of reasoning, we can show that \mathcal{V} , defined by constraints (23d)–(23e), is also a lattice. For a fixed $(v, b) \in \mathcal{V}$, $\mathcal{L}(v, b)$ is defined by the constraints (23a)–(23c). Because $\mathcal{L}(v, b)$ is a section of \mathcal{L} at (v, b) , it is also a lattice by Lemma 2.2.3 of [49]. \blacksquare

Proof of Theorem 1

Proof. To prove part (i), we use backward induction on $V_t(\bar{\mathbf{w}}_t, \mathbf{y}_t)$. The result clearly holds for stage N . For the induction hypothesis, suppose $V_{t+1}(\mathbf{w}_{t+1}, \mathbf{y}_{t+1})$ is multimodular in $\mathbf{y}_{t+1} \in \mathcal{Y}$ for any $\mathbf{w}_{t+1} \in \mathcal{W}_{t+1}$. We seek to show that $V_t(\bar{\mathbf{w}}_t, \mathbf{y}_t)$ is multimodular in $\mathbf{y}_t \in \mathcal{Y}$. This is equivalent to showing that the function

$$\begin{aligned} \Psi(\bar{\mathbf{w}}_t, v, b) &= V_t(\bar{\mathbf{w}}_t, v_1 - b, v_2 - v_1), \\ &= \min_{\mathbf{u}_t, q_t} \{c_t(\bar{\mathbf{w}}_t, \mathbf{u}_t, q_t) + \delta \mathbb{E}(V_{t+1}(\mathbf{W}_{t+1}, v_1 - b + u_t^1, v_2 - v_1 + u_t^2))\}, \\ &= \min_{\mathbf{r}} \{c_t(\bar{\mathbf{w}}_t, r_1 - v_1, r_2 - v_2, r_3 - r_2) + \delta \mathbb{E}(V_{t+1}(\mathbf{W}_{t+1}, r_1 - b, r_2 - v_1))\}, \end{aligned} \quad (24)$$

is submodular in $(v, b) \in \mathcal{V}$, such that $(r_1 - v_1, r_2 - v_2, r_3 - r_2) \in \mathcal{X}_t(v_1 - b, v_2 - v_1)$ and $\mathbf{r} \in \mathbb{R}^3$. First, we establish that the objective function of (24) is submodular in $(v, b, r) \in \mathcal{L}$, where \mathcal{L} is defined in (16). The post-decision value function $V_t^x(\bar{\mathbf{w}}_t, \mathbf{y}_{t+1})$ is

$$V_t^x(\bar{\mathbf{w}}_t, \mathbf{y}_{t+1}) = \sum_{\mathbf{w}_{t+1} \in \mathcal{W}_{t+1}} \delta \mathbb{P}^{\pi^*}(\mathbf{w}_{t+1} | \bar{\mathbf{w}}_t) V_{t+1}(\mathbf{w}_{t+1}, \mathbf{y}_{t+1}).$$

As $\delta\mathbb{P}^{\pi^*}(\mathbf{w}_{t+1}|\bar{\mathbf{w}}_t) \geq 0$, and a nonnegative affine combination of multimodular functions is multimodular by Lemma 2 (i) of [31], V_t^x is multimodular in \mathbf{y}_{t+1} . Note that $\mathbf{y}_{t+1} = \mathbf{y}_t + \mathbf{u}_t = (u_t^1 + y_t^1, y_t^2 + u_t^2)$. Using Lemma 2 (vii) in [31], we conclude that V_t^x is multimodular in $(u_t^1, y_t^1, y_t^2, u_t^2)$, or equivalently that V_t^x is submodular in $(\mathbf{v}, b, \mathbf{r})$. The one-step cost in (24) is

$$c_t(\bar{\mathbf{w}}_t, r_1 - v_1, r_2 - v_2, r_3 - r_2) = k + \theta_t^1(r_1 - v_1) + \theta_t^2(r_2 - v_2) + \varphi(|r_1 - v_1| + |r_2 - v_2|) + \nu\xi(r_1 - v_1, r_2 - v_2, r_3 - r_2), \quad (25)$$

where k is a constant that depends on $\bar{\mathbf{w}}_t$. As the absolute value function and ξ are convex, by Theorem 2.2.6 (b) of [45], we have that the terms $|r_1 - v_1|$, $|r_2 - v_2|$ and $\xi(r_1 - v_1, r_2 - v_2, r_3 - r_2)$ in (25) are submodular in $(\mathbf{v}, b, \mathbf{r})$. Moreover, the linear terms in (25) are submodular in $(\mathbf{v}, b, \mathbf{r})$ by Lemma 2.2.3 in [45]. As the sum of two submodular functions is submodular by Lemma 2.6.1 in [49], the objective function of (24) is also submodular in $(\mathbf{v}, b, \mathbf{r}) \in \mathcal{L}$. It is noted that problem (24) involves minimizing a submodular function in $(\mathbf{v}, b, \mathbf{r})$ along a section $\mathcal{L}(\mathbf{v}, b)$ of \mathcal{L} at some $(\mathbf{v}, b) \in \mathcal{V}$. Also, $\Psi(\bar{\mathbf{w}}_t, \mathbf{v}, b) > -\infty$ because $\mathcal{L}(\mathbf{v}, b)$ is a polyhedron. Then, using Theorem 2.7.6 in [49], we establish that $\Psi(\bar{\mathbf{w}}_t, \mathbf{v}, b)$ is submodular in $(\mathbf{v}, b) \in \mathcal{V}$. Therefore, $V_t(\bar{\mathbf{w}}_t, \mathbf{y}_t)$ is multimodular in $\mathbf{y}_t \in \mathcal{Y}$.

To prove Theorem 1 (ii), the dependence of V_t and Ψ on $\bar{\mathbf{w}}_t$ is suppressed to simplify notation. Let $\epsilon > 0$ and note that

$$\begin{aligned} \Delta_{2,3}\Psi(\mathbf{v}, b) &= \Psi(v_1, v_2 + \epsilon, b + \epsilon) - \Psi(v_1, v_2 + \epsilon, b) - \Psi(v_1, v_2, b + \epsilon) + \Psi(v_1, v_2, b), \\ &= V_t(y_t^1 - \epsilon, y_t^2 + \epsilon) - V_t(y_t^1, y_t^2 + \epsilon) - V_t(y_t^1 - \epsilon, y_t^2) + V_t(y_t^1, y_t^2), \\ &= -\Delta_{1,2}V_t(\mathbf{y}_t), \end{aligned} \quad (26)$$

where the last equality stems from successive forward and backward finite difference operations on V_t w.r.t. y_t^2 and y_t^1 , respectively. As submodularity implies decreasing differences by Theorem 2.2.2 in [45], we have $\Delta_{2,3}\Psi(\mathbf{v}, b) \leq 0 \Rightarrow \Delta_{1,2}V_t(\mathbf{y}_t) \geq 0$ by equation (26). Next, we show that $\Delta_{2,2}V_t(\mathbf{y}_t) \geq \Delta_{1,2}V_t(\mathbf{y}_t)$. By definition,

$$\begin{aligned} \Delta_{1,3}\Psi(\mathbf{v}, b) &= \Psi(v_1 + \epsilon, v_2, b + \epsilon) - \Psi(v_1 + \epsilon, v_2, b) - \Psi(v_1, v_2, b + \epsilon) + \Psi(v_1, v_2, b), \\ &= V_t(y_t^1, y_t^2 - \epsilon) - V_t(y_t^1 + \epsilon, y_t^2 - \epsilon) - V_t(y_t^1 - \epsilon, y_t^2) + V_t(y_t^1, y_t^2). \end{aligned} \quad (27)$$

Similarly, successive forward and backward finite difference operations on V_t yield

$$\Delta_{1,2}V_t(\mathbf{y}_t) = V_t(y_t^1 + \epsilon, y_t^2) - V_t(y_t^1 + \epsilon, y_t^2 - \epsilon) - V_t(y_t^1, y_t^2) + V_t(y_t^1, y_t^2 - \epsilon), \quad (28)$$

$$\Delta_{1,1}V_t(\mathbf{y}_t) = V_t(y_t^1 + \epsilon, y_t^2) - 2V_t(y_t^1, y_t^2) + V_t(y_t^1 - \epsilon, y_t^2). \quad (29)$$

Subtracting (29) from (28), we see that $\Delta_{1,2}V_t(\mathbf{y}_t) - \Delta_{1,1}V_t(\mathbf{y}_t) = \Delta_{1,3}\Psi(\mathbf{v}, b)$ by (27). But $\Delta_{1,3}\Psi(\mathbf{v}, b) \leq 0$, as Ψ is a submodular function. Therefore,

$$0 \leq \Delta_{1,2}V_t(\mathbf{y}_t) \leq \Delta_{1,1}V_t(\mathbf{y}_t). \quad (30)$$

Likewise, it can be shown that

$$0 \leq \Delta_{2,1}V_t(\mathbf{y}_t) \leq \Delta_{2,2}V_t(\mathbf{y}_t). \quad (31)$$

Inequalities (30) and (31) imply that V_t has increasing differences and component-wise convexity.

To prove Theorem 1 (iii), we note that \mathcal{L} is a sublattice of $\mathcal{V} \times \mathbb{R}^3$, both of which are lattices. Hence, for any $(\mathbf{v}, b) \in \mathcal{V}$, the section $\mathcal{L}(\mathbf{v}, b)$ is also a sublattice by Lemma 2.2.3 (a) of [49]. Let \sqsubseteq denote the *strong set order* defined for subsets of a lattice, where for any $A', A'' \subseteq A$, $A' \sqsubseteq A'' \Rightarrow \mathbf{a}' \wedge \mathbf{a}'' \in A'$ and $\mathbf{a}' \vee \mathbf{a}'' \in A''$ for all $\mathbf{a}' \in A'$ and $\mathbf{a}'' \in A''$ (see Section 2.4 of [49]). As $\mathcal{L}(\mathbf{v}, b)$ is a sublattice, it is also an increasing set function in $(\mathbf{v}, b) \in \mathcal{V}$ with respect to \sqsubseteq by Theorem 2.4.5(a) of [49]. It is easy to verify that $\mathcal{L}(\mathbf{v}, b)$ is nonempty for any $(\mathbf{v}, b) \in \mathcal{V}$. Therefore, we conclude that \mathbf{x}_t^* is monotone decreasing in $\mathbf{y}_t \in \mathcal{Y}$ by using Theorem 2.8.2 in [49]. Next, we derive the bounds on $\Delta_1 u_t^{1*}$ and $\Delta_2 u_t^{1*}$ (their dependence on $(\bar{\mathbf{w}}_t, \mathbf{y}_t)$ is suppressed for simplicity). Let $J_t(u_t^1, y_t^1, y_t^2, u_t^2)$ be the objective function of (9) for a fixed $q_t \in [-\beta, \beta]$. By definition,

$$V_t(y_t^1, y_t^2) = \min_{u_t^1, u_t^2} \{ J_t(u_t^1, y_t^1, y_t^2, u_t^2) : 0 \leq u_t^1 + y_t^1 \leq \alpha_1, 0 \leq u_t^2 + y_t^2 \leq \alpha_2 \}.$$

Next, J_t is minimized sequentially with respect to u_t^2 and u_t^1 , respectively. Minimizing J_t over the set of feasible u_t^2 values, and using arguments similar to those in the proof of part (i), we obtain

$$\tilde{J}_t(u_t^1, y_t^1, y_t^2) = \min_{u_t^2} \{ J_t(u_t^1, y_t^1, y_t^2, u_t^2) : 0 \leq u_t^1 + y_t^1 \leq \alpha_1, 0 \leq u_t^2 + y_t^2 \leq \alpha_2 \},$$

which is multimodular in (u_t^1, y_t^1, y_t^2) . Next, minimizing \tilde{J}_t over the set of feasible u_t^1 values gives

$$V_t(y_t^1, y_t^2) = \min_{u_t^1} \{ \tilde{J}_t(u_t^1, y_t^1, y_t^2) : 0 \leq u_t^1 + y_t^1 \leq \alpha_1 \},$$

which is multimodular in (y_t^1, y_t^2) . Applying Corollary 1 (ii) of [31], we obtain $-1 \leq \Delta_1 u_t^{1*} \leq \Delta_2 u_t^{1*} \leq 0$. Similar bounds on $\Delta_1 u_t^{2*}$ and $\Delta_2 u_t^{2*}$ are obtained by minimizing J_t over u_t^1 , followed by u_t^2 , and applying Theorem 1 (ii) of [31]. \blacksquare

Proof of Proposition 5

Proof. Consider three storage capacity vectors α_1, α_2 and α_3 , such that $\alpha_1 < \alpha_2 < \alpha_3$ and $\alpha_2 = \eta\alpha_1 + (1 - \eta)\alpha_3$, where $\eta \in [0, 1]$. We seek to show that $z_{\alpha_2} \leq \eta z_{\alpha_1} + (1 - \eta)z_{\alpha_3}$. Consider a state $\mathbf{s}_t = (\mathbf{w}_t, \mathbf{y}_t) \in \mathcal{S}_t$. Let $\mathbf{x}_t^{k*} = (u_t^{k*}, q_t^{k*})$ be the optimal solution vector of (8) for $\alpha = \alpha_k$, where $k \in \{1, 2, 3\}$. Construct a policy $\tilde{\pi} = (\tilde{\mathbf{x}}_t : t \in T')$, such that $\tilde{\mathbf{u}}_t = \eta u_t^{1*} + (1 - \eta)u_t^{3*}$ and $\tilde{q}_t = \eta q_t^{1*} + (1 - \eta)q_t^{3*}$. Multiply both sides of the constraints in $\mathcal{X}_t(\mathbf{y}_t; \alpha_1)$ by η and those in $\mathcal{X}_t(\mathbf{y}_t; \alpha_3)$ by $(1 - \eta)$, and add the corresponding constraints to obtain the inequalities

$$\begin{aligned} -\min\{\tau_d, \mathbf{y}_t\} &\leq \eta u_t^{1*} + (1 - \eta)u_t^{3*} \leq \min\{\tau_c, \alpha_2 - \mathbf{y}_t\}, \\ -\beta &\leq \eta q_t^{1*} + (1 - \eta)q_t^{3*} \leq \beta, \end{aligned}$$

which shows that $\tilde{\pi}$ is a feasible, but not necessarily optimal, policy of (8) for $\alpha = \alpha_2$. Furthermore, it can be verified that

$$c_t(\mathbf{s}_t, \tilde{\mathbf{x}}_t) = \eta c_t(\mathbf{s}_t, \mathbf{x}_t^{1*}) + (1 - \eta)c_t(\mathbf{s}_t, \mathbf{x}_t^{3*}), \quad t \in T'. \quad (32)$$

Summing the one-step costs in (32) and taking the expectation of this sum gives

$$z_{\alpha_2} \leq \mathbb{E}_{\tilde{\pi}} \left(\sum_{t \in T'} c_t(\mathbf{s}_t, \tilde{\mathbf{x}}_t) \right) = \eta z_{\alpha_1} + (1 - \eta) z_{\alpha_3},$$

which completes the proof of convexity.

Next, to show monotonicity, consider two storage capacity vectors α_1 and α_2 , such that $\alpha_2 = \alpha_1 + \Gamma$ where $\Gamma > \mathbf{0}$. Let $\mathbf{w} = (\mathbf{w}_t : t \in T)$ be a realization of the exogenous process, and π_1 and π_2 denote the optimal policies of (8) for $\alpha = \alpha_1$ and $\alpha = \alpha_2$, respectively. Let $z_{\alpha_1}(\mathbf{w})$ and $z_{\alpha_2}(\mathbf{w})$ be the total costs incurred by along the trajectory \mathbf{w} using π_1 and π_2 , respectively. Without loss of generality, suppose $\mathbf{y}_1 = \mathbf{0}$ for both policies. Let $\mathbf{s}_t^1 = (\mathbf{w}_t, \mathbf{y}_t^1)$ be the state of the process at stage t under π_1 . Then, π_1 is a feasible policy of (8) when $\alpha = \alpha_2$, as $\mathbf{u}_t^1 \leq \alpha_1 - \mathbf{y}_t^1 \Rightarrow \mathbf{u}_t^1 \leq \alpha_1 + \Gamma - \mathbf{y}_t^1 = \alpha_2 - \mathbf{y}_t^1$ as $\Gamma > \mathbf{0}$ and $q_t^1 \in [-\beta, \beta]$; therefore, $z_{\alpha_1}(\mathbf{w}) \geq z_{\alpha_2}(\mathbf{w})$. As \mathbf{w} is any feasible realization in \mathcal{W} , we can conclude that

$$z_{\alpha_1} = \sum_{\mathbf{w} \in \mathcal{W}} z_{\alpha_1}(\mathbf{w}) \mathbb{P}(\mathbf{W} = \mathbf{w}) \geq \sum_{\mathbf{w} \in \mathcal{W}} z_{\alpha_2}(\mathbf{w}) \mathbb{P}(\mathbf{W} = \mathbf{w}) = z_{\alpha_2},$$

which completes the proof. ■